PHYSICAL REVIEW B VOLUME 5, NUMBER 7 1 APRIL 1972

Theory of Critical-Point Scattering and Correlations. II. Heisenberg Models

Douglas S. Ritchie and Michael E. Fisher
Baker Laboratory, Cornell University, Ithaca, New York 14850
(Received 4 September 1971)

The spin-spin correlation functions and the critical-scattering intensity for Heisenberg models of general spin, $S=\frac{1}{2}$ to ∞, on the sc, bcc, and fcc lattices are studied on the basis of high-temperature series expansions along the lines developed in Paper I [M. E. Fisher and R. J. Burford, Phys. Rev. 156, 583 (1967)]. Subject to increased uncertainties for low spin, it is concluded that the exponents $\gamma = 1.375^{+0.02}_{-0.01}$, $2\nu = 1.405^{+0.02}_{-0.01}$, and $\eta = 0.043 \pm 0.014$ describe all lattices and all spin. Explicit formulas are presented for the susceptibility/zero-angle scattering $\chi_0(T)$, for the inverse correlation length $\kappa_1(T)$, for the effective interaction range $r_1(T)$, and using the Fisher-Burford approximant, for the total scattering $\hat{\chi}(\vec{k}, T)$. The shape parameter ϕ_c attains the "universal" value $\phi_c \simeq 0.11$ for large spin but shows signs of spin dependence (and lattice dependence) for low spin. At fixed $\vec{k}$ the scattering is predicted to display a maximum *above* T_c determined by $\kappa_1(T_{max})/k \simeq 0.10$ (for $S \gtrsim 2$) to 0.15. A detailed study is made of the structure dependence of the critical-point correlations $\langle S_0^z S_{\vec{l}}^z \rangle_c$ for various models. This leads to the revised, universal estimate $\phi_c \simeq 0.15$ for all three cubic lattice, spin-$\frac{1}{2}$ Ising models. The results are compared briefly with various experiments which support $\eta \gtrsim 0.05$.

I. INTRODUCTION

Near the critical point of a many-body system there is a large increase in the scattering intensity in certain directions. In the case of a ferromagnet the critical scattering, which can be observed with neutrons, occurs in the forward direction and is associated with large-scale fluctuations in the local magnetization. The general nature of this magnetic critical scattering has been quite well understood since the work of Van Hove,[1] who adapted the classical theory of Ornstein and Zernike.[2] If one restricts attention to the quasielastic scattering (which in the case of neutron scattering must be obtained experimentally by taking careful account of the inelastic nature of most of the scattering), and uses the first Born approximation (which is normally quite adequate if appropriate experimental precautions are taken), one finds that the scattering intensity is essentially proportional to the Fourier transform of the spin-pair correlations[1,2]

$$\Gamma^{\mu\nu}(\vec{r} - \vec{r}'; H, T) \propto \langle (S_{\vec{r}}^{\mu} - \langle S_{\vec{r}}^{\mu} \rangle)(S_{\vec{r}'}^{\nu} - \langle S_{\vec{r}'}^{\nu} \rangle) \rangle \ . \quad (1.1)$$

As is well known, the calculation of the intensity of the critical scattering thus reduces to a study of the pair-correlation functions and especially their long-range slow spatial decay in the critical region.

In Paper I of this series[3] such a study was performed for the spin-$\frac{1}{2}$ Ising model of a ferromagnet, which also serves as a model of a lattice gas, a binary fluid, an anisotropic antiferromagnet, and, most successfully, of a binary alloy such as beta-brass. That study was particularly motivated by exact theoretical results for the plane-square Ising model, which revealed unequivocally the defects of the classical Ornstein-Zernike theory.[2,3] The ideas involved have been reviewed quite extensively[2,3] and will not be reiterated here. The aim of the present paper is to reproduce the calculations of Paper I for the Heisenberg model of a ferromagnet in order to obtain numerically accurate and analytically convenient approximants for the scattering intensity (and correlation functions) at all temperatures above critical (and in zero field). Attention is restricted to the nearest-neighbor fully isotropic Heisenberg ferromagnet but all spins from $S=\frac{1}{2}$ to $S=\infty$ are considered. In addition, the results for the classical limit will be applicable to the corresponding antiferromagnets. Incidentally, we have also improved aspects of the original calculations for the Ising model. (See Secs. V B and VI A.)

The two-dimensional Heisenberg model is not considered here. It has been proven that this model has no spontaneous magnetization and no long-range order.[4] Nevertheless, there remains the possibility of a transition at which the initial susceptibility diverges.[5] However, the uncertainties attached to this crucial point suggest that attempts at a detailed numerical calculation of the correlation functions in the presumed critical region would be premature.

As in Paper I, our work is based on the numerical analysis and extrapolation of high-temperature series expansions for the susceptibility, for the second and higher moments of the correlation functions, and for the individual correlation functions themselves. The available series (see Sec. III) are, unfortunately, appreciably shorter than for the Ising model so the numerical results are correspondingly less precise and less certain. Nevertheless, the dominant features and various important details can be established with confidence: In particular, we find a small but definitely nonzero value of the exponent η and, in addition, the maximum in the scattering intensity at fixed angle occurs *above* the critical temperature T_c. Graphs of the various quantities of interest are presented in Sec. VI. The final result for the scattering intensity is expressed in

terms of the exponents η and ν and an explicit formula for the inverse correlation range $\kappa_1(T)$. (See Summary in Sec. VI.)

The layout of the rest of the paper is as follows: In Sec. II the notation and certain preliminary relations are presented. For the most part the reader is referred to Paper I except where specific differences arise. The numerical extrapolation of the susceptibility and second-moment series is discussed in Sec. IV. The individual correlation functions are extrapolated in Sec. V. The scattering approximants are developed in Sec. VI and the results discussed and compared briefly with experiments in Sec. VII.

II. NOTATION AND FORMAL RELATIONS

We shall use the same notation as in Paper I, unless stated otherwise. The few exceptions arise because we are dealing with the Heisenberg model. The reader should refer to Secs. II–VI of Paper I to familiarize himself with the notation and in order to understand the theory behind the Fisher-Burford approximants for the correlation functions and their Fourier transforms. (We also draw attention to the glossary of symbols in Paper I.)

A. Model

In this paper we study the critical properties of the isotropic nearest-neighbor Heisenberg model above the critical temperature. In order to treat general values of the spin, all properties will be normalized so as to pass continuously over to the classical case $S=\infty$. The Hamiltonian for the Heisenberg model of spin S will be written as

$$\mathcal{H}=-\frac{J}{S^2}\sum_{(ij)}\vec{S}_i\cdot\vec{S}_j-\frac{mH}{S}\sum_{i=1}^{N}S_i{}^z\,, \tag{2.1}$$

where $\vec{S}_i\equiv(S_i{}^x, S_i{}^y, S_i{}^z)$ is the spin operator on the ith lattice site ($i=1,\ldots,N$), $m(=g\mu_B S)$ is the magnetic moment of the spin, J is the exchange parameter, H is the external magnetic field which is applied in the z direction, and (ij) here denotes that the sum extends over all nearest-neighbor pairs of sites.

We shall assume that the exchange parameter J is positive, that is, the model is one of a ferromagnet. The previous result that the zero-field scattering for an Ising antiferromagnet about the superlattice-point is identical to the scattering from the ferromagnet about zero-momentum transfer[3] holds now only for the classical Heisenberg model ($S=\infty$), but is not valid for finite spin owing to the lack of commutation of the relevant operators.

The magnetization is defined as

$$M^z=\frac{m}{S}\sum_{i=1}^{N}\langle S_i{}^z\rangle\,, \tag{2.2}$$

where the angular brackets denote the standard statistical average calculated with (2.1). In zero field above the critical point, there is no long-range order and the correlation function may conveniently be defined as

$$\Gamma^{\mu\nu}(\vec{r})=[3/S(S+1)]\,\langle S_0^{\mu}S_{\vec{r}}^{\nu}\rangle\quad(H=0)\,. \tag{2.3}$$

With these definitions, the susceptibility-fluctuation theorem takes the form

$$\chi_0(T)=\left(\frac{3S}{S+1}\right)\left(\frac{k_BT}{m^2}\right)\chi^{zz}(T)=\sum_{\vec{r}}\Gamma^{zz}(\vec{r})\,, \tag{2.4}$$

where $\chi^{zz}=\partial M^z/\partial H$ while $\chi_0(T)$ is the basic reduced susceptibility which approaches unity as $T\to\infty$ (for all S). For the isotropic Heisenberg model, above the critical temperature and in zero field we have the further simplification

$$\Gamma^{\mu\nu}(\vec{r})=\tfrac{1}{3}\delta_{\mu\nu}\Gamma(\vec{r})\,,\quad \Gamma^{\mu\mu}(\vec{0})=1\,, \tag{2.5}$$

where

$$\Gamma(\vec{r})=[3/S(S+1)]\,\langle\vec{S}_{\vec{0}}\cdot\vec{S}_{\vec{r}}\rangle=3\Gamma^{zz}(\vec{r})\,. \tag{2.6}$$

B. Scattering Cross Section

For simplicity consider a beam of unpolarized neutrons incident upon the system of localized spins, fixed to a lattice. The scattering is caused by the magnetic interaction between the neutron dipole moment and the moments of the lattice spins. In the quasielastic Born approximation, the scattered intensity $(\partial\sigma/\partial\Omega)$ in a given direction is found to be proportional to the spatial Fourier transform of the correlation function.[1,6,7] We introduce a reduced scattered intensity which is normalized by the scattered intensity from a lattice of paramagnetic spins, namely,

$$\hat{\chi}(\vec{k})=\left(\frac{\partial\sigma}{\partial\Omega}\right)\Big/\left(\frac{\partial\sigma}{\partial\Omega}\right)_{\text{ideal}}=1+\hat{\Gamma}^{zz}(\vec{k})\,, \tag{2.7}$$

where the Fourier transform is defined as in Paper I, namely,

$$\hat{\Gamma}^{zz}(\vec{k})=\sum_{r\neq0}e^{i\vec{k}\cdot\vec{r}}\,\Gamma^{zz}(\vec{r})\,, \tag{2.8}$$

and $\vec{k}$ is the momentum transfer to the scattered neutron.

C. Further Notation

The notation now parallels that in Paper I, except that the correlation function $\hat{\Gamma}(\vec{k})$ in Paper I should, for the isotropic Heisenberg model, always be replaced by $\hat{\Gamma}^{zz}(\vec{k})$. In particular, the spherical moments of the correlation function are defined by

$$\mu_t(T)=\sum_{r\neq0}(r/a)^t\,\Gamma^{zz}(\vec{r})\,. \tag{2.9}$$

At a fixed temperature above the critical point, and for sufficiently small $(ka)^2$ the scattering function $\hat{\chi}(k, T)$ should have a convergent expansion of the form

$$1/\hat{\chi}(k, T) = [\chi_0(T)]^{-1}[1 + \Lambda_2(T)(ka)^2 - \Lambda_4(T)(ka)^4 + \cdots], \tag{2.10}$$

where

$$\Lambda_2(T) = (\kappa_1 a)^{-2} = \mu_2(T)/2d\chi_0(T) . \tag{2.11}$$

It will be remembered that the Ornstein-Zernike hypothesis asserts that the expansion (2.10) is valid up to and *at* the critical point, so that at $T = T_c$,

$$\hat{\chi}_c(k) \approx \hat{D}/(ka)^2 \qquad (ka \to 0) . \tag{2.12}$$

More generally, however, such an expansion is no longer valid and one must expect[2,3]

$$\hat{\chi}_c(k) \approx \hat{D}/(ka)^{2-\eta} \qquad (ka \to 0) . \tag{2.13}$$

In addition to the exponent η which is expected to be positive, the exponents γ and ν describe the asymptotic behavior in the critical region of the susceptibility as

$$\chi_0(T) \sim [1 - (T_c/T)]^{-\gamma} \qquad (T \to T_c+) \tag{2.14}$$

and the effective (inverse) range of correlation as

$$\kappa_1(T) = [\Lambda_2(T)a^2]^{-1/2} \sim [1 - (T_c/T)]^{\nu} \quad (T \to T_c+) . \tag{2.15}$$

These exponents are expected to be related by[2,3] $(2 - \eta)\nu = \gamma$.

D. Approximant for Scattering

Fisher and Burford[2] proposed the following approximant for the scattering function:

$$\hat{\chi}(\vec{k}, T) \simeq \chi_0(T) \frac{[1 + \phi^2\Lambda_2(T)\hat{K}^2(\vec{k})a^2]^{\eta/2}}{[1 + \psi\Lambda_2(T)\hat{K}^2(\vec{k})a^2]} , \tag{2.16}$$

where

$$\hat{K}^2(\vec{k}) = 2d[1 - q^{-1}\textstyle\sum_{\vec{\delta}} e^{i\vec{k}\cdot\vec{r}}] = k^2[1 + O(k^2a^2)] , \tag{2.17}$$

in which d and q are the dimensionality and coordination number of the lattice and $\vec{\delta}$ runs over the set of nearest-neighbor lattice vectors. [In Paper I $\hat{K}(\vec{k})$ was denoted by $K(\vec{k})$ but we have modified the notation to avoid confusion with the expansion variable $J/k_BT = K$, see below.] This approximant embodies most of the features of the exact results for the two-dimensional Ising model that are expected to be generally valid. The function $\psi(T)$ is chosen so that at high temperatures the denominator has two simple poles at $k = \pm i\kappa$, where $\kappa(T)$ is the true inverse range of correlation (corresponding to an asymptotic decay of correlation as $e^{-\kappa r}$).[2,3] Second, $\phi(T)$ is chosen so that the expansion for small $(ka)^2$ of $1/\hat{\chi}(\vec{k}, T)$ will be identical with the exact expansion (2.10) up to first order in $(ka)^2$. This implies the relation

$$\psi(T) = 1 + \tfrac{1}{2}\eta\phi^2(T) . \tag{2.18}$$

Finally, the critical value of $\phi(T)$ is chosen to give the correct amplitude of scattering at the critical point. Thus at $T = T_c$ the approximant (2.16) reduces to

$$\hat{\chi}_c(\vec{k}) \approx \frac{[(\kappa_1 a)^{2-\eta}\chi_0]_{T=T_c}\phi_c^{\eta}/\psi_c}{(ka)^{2-\eta}} \tag{2.19}$$

as $ka \to 0$, and so ϕ_c can be determined to match the amplitude $\hat{D}$ in (2.13).

III. SERIES FOR HEISENBERG MODEL

Since there is no analytic solution of the Heisenberg model available, exact series expansions will be used to study the various properties of interest. We consider, in particular, high-temperature series in the variable

$$K = J/k_BT \tag{3.1}$$

for the susceptibility, the second moment of the correlations, and the correlation functions for various lattice vectors $\vec{r}$.

In this section the sources of these series are explained. The series are given in Tables I–III. We consider the face-centered-cubic (fcc), the body-centered-cubic (bcc), and the simple-cubic (sc) lattices. To avoid undue tabulation we consider explicitly only the spin values $S = \frac{1}{2}$, 1, $\frac{3}{2}$, $\frac{5}{2}$, and ∞. The results for other values follow to sufficient accuracy by interpolation in the variable $1/S(S+1)$ which is what enters the general expressions.[8]

A. Susceptibility Series

The coefficients of the susceptibility series are normalized by the definition

$$\chi_0(K) = \sum_{n=0}^{\infty} a_n K^n . \tag{3.2}$$

With this normalization we always have

$$a_0 = 1 \quad \text{and} \quad a_1 = q(S+1)/3S , \tag{3.3}$$

with $q = 6$, 8, and 12 for sc, bcc, and fcc, respectively. It follows that the mean-field approximation for the critical temperatures is given by

$$k_BT_c^{\text{mf}} = k_BT_0 = qJ(S+1)/3S . \tag{3.4}$$

Rushbrooke and Wood[8] calculated the coefficients a_n to sixth order for general spin; Stephenson, Pirnie, Wood, and Eve[9] have obtained the seventh-order term. For the spin-$\frac{1}{2}$ model, the series have been extended to tenth order for the loose-packed lattices and ninth order for the fcc lattice, by Baker *et al.*[10,11] In addition, the series for the $S = \infty$ classical model has been extended further by Jasnow and Wortis[12] to ninth order for the loose-packed lattices and eighth order for the fcc lattice. Recently the fcc series has been extended to tenth order by Moore.[13(a),(b)]

The coefficients for these susceptibility series are listed in Table I.

TABLE I. Susceptibility series coefficients a_n.

n	fcc	bcc	sc
		$S=\frac{1}{2}$	
1	12	8	6
2	120	48	24
3	1104	277.3333	88
4	9780	1533.3333	330
5	85073.600	8406.4000	1248.8000
6	731680.800	45314.6667	4401.7333
7	6237020.952	242341.0794	15287.0095
8	52772446.05	1283099.809	55337.5429
9	443850499.4	6776582.797	198243.2423
10		35571676.39	674141.7367
		$S=1$	
1	8	5.3334	4
2	56.6667	23.5556	12.3333
3	380.4445	101.9259	36.4444
4	2481.0185	421.4198	103.8426
5	15891.6346	1727.1309	293.4469
6	100574.8113	6958.0542	813.3398
7	631067.476	27892.372	2238.5293
		$S=\frac{3}{2}$	
1	6.6667	4.4444	3.3333
2	40	16.7901	8.8889
3	229.1139	62.3685	22.9246
4	1278.6618	222.3137	56.9441
5	7019.0057	785.8202	140.1383
6	38096.4579	2731.8190	338.8217
7	205085.045	9452.8525	814.1216
		$S=\frac{5}{2}$	
1	5.6000	3.7333	2.8000
2	28.5227	12.0462	6.4213
3	139.3037	38.3260	14.3189
4	664.2970	117.2651	30.7881
5	3119.3376	356.1623	65.5964
6	14491.9231	1064.6229	137.4341
7	66803.2293	3168.3769	286.2656
		$S=\infty$	
1	4	2.6667	2
2	14.6667	6.2222	3.3333
3	51.7333	14.3407	5.4222
4	178.4593	31.8617	8.5185
5	606.7454	70.3116	13.2670
6	2042.1004	152.8116	20.3360
7	6821.9528	330.7434	30.9990
8	22659.3609	709.9936	46.8667
9	74921.3032	1519.8070	70.6068
10	246802.5462		

TABLE II. Series coefficients for the moments of the correlation function. For definition of the coefficients $m_n(t)$ see Eq. (3.5).

n	fcc	bcc	sc
		(A) Second moment $t=2$	
		$S=\frac{1}{2}$	
1	12	8	6
2	276	120	66
3	4504	1253.3333	492
4	60080	10325.3333	2728
5	716302.4000	76820.2667	13428
6	7964389.8667	534713.2444	62943.7333
		$S=1$	
1	8	5.3333	4
2	126	55.5556	31
3	1407.1111	400	161.3333
4	13269.9074	2407.4938	681.8426
5	113736.3654	13189.4453	2598.8642
6	916100.6846	67820.7252	9275.0188
		$S=\frac{3}{2}$	
1	6.6667	4.4444	3.3333
2	88.1481	39.0123	21.8519
3	826.3704	236.3274	96.0384
4	6598.4941	1214.5466	350.2210
5	48087.9796	5694.1497	1156.4007
6	330135.6829	25127.1547	3581.3859
		$S=\frac{5}{2}$	
1	5.6000	3.7333	2.8000
2	62.4960	27.7262	15.5680
3	494.5080	141.9766	57.9790
4	3351.0799	622.5585	181.5808
5	20781.2099	2493.9379	516.2252
6	121598.0026	9423.5424	1379.2376
		$S=\infty$	
1	4	2.6667	2
2	32	14.2222	8
3	181.5111	52.2667	21.4222
4	885.3333	165.6099	48.7111
5	3959.3972	479.9116	100.7337
6	16728.5269	1314.0260	196.1286
7	67885.8962	3453.2284	365.7050
8	267307.9501	8805.2527	660.4992
9	1028186.2491	21925.4904	1163.5584
10	3881417.5558		
		(B) Fourth moment $t=4$	
		$S=\infty$	
1	4	2.666 666 67	2
2	85.333 333 3	37.925 925 9	21.333 333 3
3	821.511 111	241.896 296	101.422 222
4	5796.740 74	1115.865 02	343.229 630
5	34499.249 1	4325.881 40	964.733 686
6	184184.314	15010.879 5	2409.810 32
7	911579.099	48231.670 3	5547.327 40
8	4265876.89	146414.162	12024.463 2
9		425450.198	24888.178 6

TABLE III. Series coefficients for the correlation function. For definition of the coefficients $q_n(\vec{r})$ see Eq. (3.7).

(A) Nearest-neighbor correlation or energy series $\vec{r}=\vec{\delta}$
Note: $q_1(\vec{\delta}) \equiv 1$.

n	fcc	bcc	sc
		$S=\frac{1}{2}$	
2	3	−1	−1
3	1.6667	2.3333	−3
4	−11.6667	5	11.6667
5	75	17	30.7333
6	1 123.8889	−34.3778	−157.2667
7	6 208.7016	463.2476	−172.0667
8	24 174.1619	−1103.0127	1995.0444
9	114 921.8577	9451.3146	795.0360
		$S=1$	
2	2.4167	−0.2500	−0.2500
3	6.1111	3.4444	0.3333
4	19.2940	−1.0764	0.1273
5	71.6698	16.6019	3.3414
6	295.3278	−6.0532	−1.5593
7	1 314.8757	127.3582	5.3604
		$S=\frac{3}{2}$	
2	2.1111	−0.1111	−0.1111
3	5.3342	2.9062	0.6016
4	15.9218	−0.4797	−0.0681
5	52.0210	11.6202	1.9122
6	183.3319	−2.4879	−0.3904
7	689.3384	64.8619	4.1212
		$S=\frac{5}{2}$	
2	1.8267	−0.0400	−0.0400
3	4.2739	2.2952	0.6028
4	11.4318	−0.1467	−0.0355
5	32.8567	7.2456	1.1793
6	100.7318	−0.6305	−0.0990
7	326.0232	30.1335	2.1414
		$S=\infty$	
2	1.3333	0	0
3	2.3778	1.2667	0.377 78
4	4.7407	0	0
5	10.0913	2.2138	0.371 78
6	22.7727	0	0
7	53.8991	4.9374	0.380 52
8	132.2585	0	0
9	333.6282	12.7521	0.477 56
10	860.2701		

(B) Correlation function for $S=\infty$
Note: $q_1(\vec{r})=1$ for $\vec{r}=\vec{\delta}$. All coefficients otherwise not listed vanish identically.

(1) fcc $S=\infty$

n	$\vec{r}=(1,1,0)$	$\vec{r}=(2,0,0)$	$\vec{r}=(2,2,0)$
2	1.333 333 333	1.333 333 333	0.333 333 333
3	2.377 777 778	2.666 666 667	1.333 333 333
4	4.740 740 741	5.451 851 852	4.177 777 778
5	10.091 287 47	12.088 888 89	11.160 493 82
6	22.772 674 89	28.100 552 61	28.496 907 70
7	53.899 069 56	67.576 826 17	72.509 911 81
8	132.258 525 3	167.315 489 7	186.190 606 8
9	333.628 207 5	424.525 246 1	484.115 040 0
10	860.270 054 8	1099.204 139	1275.186 156

TABLE III. (*Continued*)

n	$\vec{r}=(2,2,1)$	$\vec{r}=(2,2,2)$	$\vec{r}=(3,1,0)$
2	0.666 666 667	0	0
3	2	0.666 666 667	1
4	4.948 148 148	2.666 666 667	3.555 555 56
5	11.960 493 82	8.385 185 185	10.108 641 97
6	29.047 477 95	24.237 037 04	27.140 740 74
7	71.676 710 96	66.978 624 33	71.487 524 97
8	180.357 091 9	181.534 350 7	187.770 615 4
9	462.554 070 1	489.578 346 8	495.768 555 5
10	1 206.739 754	1323.064 146	1320.060 760

n	$\vec{r}=(3,2,1)$	$\vec{r}=(3,3,0)$
3	0.333 333 333	0.111 111 111
4	1.925 925 926	0.888 888 889
5	7.032 098 765	4.422 222 222
6	21.730 041 15	16.134 979 42
7	62.538 091 31	51.294 462 08
8	174.322 066 2	152.792 422 7
9	479.588 722 9	440.440 463 1
10	1314.861 045	1249.027 058

(2) bcc $S=\infty$

n	$\vec{r}=\frac{1}{2}(1,1,1)$
3	1.266 666 67
5	2.213 756 64
7	4.937 410 89
9	12.752 118 9

n	$\vec{r}=(1,0,0)$	$\vec{r}=(1,1,0)$	$\vec{r}=(1,1,1)$
2	1.333 333 33	0.666 666 67	0.333 333 33
4	1.896 296 29	1.837 037 03	1.511 111 11
6	3.801 622 57	4.256 037 62	4.227 936 51
8	9.229 812 53	10.795 837 2	11.471 595 5

n	$\vec{r}=\frac{1}{2}(3,1,1)$	$\vec{r}=\frac{1}{2}(3,3,1)$	$\vec{r}=\frac{1}{2}(3,3,3)$
3	1.0	0.333 333 33	0.111 111 11
5	2.750 617 29	1.945 679 01	1.162 962 96
7	7.072 490 69	6.497 597 49	5.182 198 70
9	19.273 295 8	19.803 950 1	18.176 815 2

(3) sc $S=\infty$

n	$\vec{r}=(1,0,0)$
3	0.377 777 78
5	0.371 781 31
7	0.380 524 40
9	0.477 555 80

n	$\vec{r}=(1,1,0)$	$\vec{r}=(2,0,0)$	$\vec{r}=(4,0,0)$
2	0.666 666 67	0.333 333 33	0.000 000 00
4	0.503 703 70	0.400 000 00	0.037 037 03
6	0.502 051 20	0.585 138 15	0.154 732 51
8	0.588 090 14	0.713 146 00	0.458 809 85

n	$\vec{r}=(1,1,1)$	$\vec{r}=(2,1,0)$	$\vec{r}=(3,0,0)$
3	0.666 666 67	0.333 333 33	0.111 111 11
5	0.533 333 33	0.513 580 25	0.274 074 07
7	0.614 509 11	0.669 888 30	0.583 021 76
9	0.782 381 08	0.884 467 61	0.906 968 37

B. Moments of Correlation Function

We define the coefficients of the series for the tth spherical moment of the correlation function by

$$\mu_t(K) = \sum_{n=1}^{\infty} m_n^{(t)} K^n \ . \tag{3.5}$$

With this normalization we always have

$$m_1^{(2)} = q(S+1)/3S \ . \tag{3.6}$$

The series for the second moment has been calculated up to sixth order for general spin by Burford.[14] For the classical model Jasnow[12] has calculated the series to ninth order for the bcc and sc lattices and to eighth order for the fcc lattice. Again, Moore has extended the series to tenth order for the fcc classical model.[13(a),(b)]

The fourth-moment series for the classical model was especially calculated for this work to ninth order for the bcc and sc lattices and to eighth order for the fcc lattice, using a program written by Jasnow.[12] Moore has extended the fcc series to tenth order.[13(a),(b)]

The coefficients of the moment series are given in Table II.

C. Correlation Functions

The correlation function in zero field can be expressed as a power series in K with coefficients $q_n(\vec{r})$ which are functions of position, explicitly

$$\Gamma^{zz}(\vec{r}) = \frac{S+1}{3S} \sum_{n=1}^{\infty} q_n(\vec{r}) K^n \ . \tag{3.7}$$

With this normalization we have $q_1(\vec{\delta}) = 1$ (where $\vec{\delta}$ is a nearest-neighbor vector).

The internal energy of the system is directly proportional to the nearest-neighbor correlation function, that is,

$$\begin{aligned} U(T) &= -\tfrac{1}{2} qJ(1+S^{-1})\, \Gamma^{zz}(\vec{\delta}) \\ &= -\tfrac{1}{6} qJ(1+S^{-1})^2 \sum_{n=1}^{\infty} q_n(\vec{\delta}) K^n . \end{aligned} \tag{3.8}$$

The magnetic specific heat in zero field is the temperature derivative of the internal energy so that

$$C_0/k_B = \tfrac{1}{6} q(1+S^{-1})^2 K \sum_{n=1}^{\infty} n q_n(\vec{\delta})\, K^n \ . \tag{3.9}$$

For general spin Rushbrooke and Wood have obtained the first five terms in the specific-heat series.[8] Stephenson *et al.* have obtained the sixth term.[9] Baker *et al.*[11] have calculated nine terms of the specific-heat series for the spin-$\frac{1}{2}$ model.

For the classical model the coefficients $q_n(\vec{r})$ of the series for the correlation function were calculated using Jasnow's program[12] for lattice sites with $r \lesssim 3a$. For the loose-packed lattices the series was obtained to ninth order; for the fcc lattices, to eighth order, and extended to tenth order by Moore.[13] Collins[15] has recently calculated the first four orders of the correlation-function expansion for general spin; we have not used his results explicitly but they confirm Burford's coefficients for the second moment to this order.

The coefficients of the energy series for general spin and for the correlation function for several lattice vectors $\vec{r}$ for the spin-∞ model are given in Table III.

IV. ANALYSIS OF SERIES

In this section we present a systematic extrapolation of the series for the susceptibility and moments of the correlation function. We shall analyze series for the three lattices and for the spin values $S = \frac{1}{2}$, 1, $\frac{3}{2}$, $\frac{5}{2}$, and ∞: The dependence of the various critical properties on spin and coordination number will be examined. Since most of these properties are singular at the critical point, either diverging as a power law or, if finite, having branch points, care must be taken in the extrapolation. The two methods used—the ratio method and Padé approximant techniques—are well described in the literature.[2(b),16]

A. Susceptibility Series

We assume that the susceptibility can be described in the critical region by

$$\chi_0(K) = A(K)\ [1 - (K/K_c)]^{-\gamma} , \tag{4.1}$$

where $A(K)$ is a function which is finite at the critical point and, hopefully, not strongly singular there.

Since the susceptibility series are better behaved than the series for the moments or the correlation functions, the critical points $K_c = J/k_B T_c$ have first been determined from the susceptibility series and then used in the analysis of the other series.

Estimates of the critical point and corresponding estimates for the exponent γ were obtained by extrapolating the ratios and from the Padé approximants to the logarithmic derivatives.[2(b),16] A typical plot of the ratios and a sample table of Padé approximant roots and residues are given in Fig. 1 and Table IV, respectively. Table V lists the values estimated for the exponent γ from each of the series, using these two methods, together with their apparent uncertainties. By contrast with similar results for the Ising model these uncertainties are quite large.

Baker *et al.*[11] have concluded that for the spin-$\frac{1}{2}$ model all the lattices have an exponent $\gamma = 1.43 \pm 0.01$. Jasnow and Wortis[12] and Joyce and Bowers[17] both conclude that $\gamma = 1.38 \pm 0.02$ for the classical ($S = \infty$) model for all three lattices (revising the original estimate $\gamma \simeq 1.33$ of Domb and Sykes[18]). More recently Bowers and Woolf[19] have conjectured that $\gamma = 1.375$ independently of spin and lattice. For

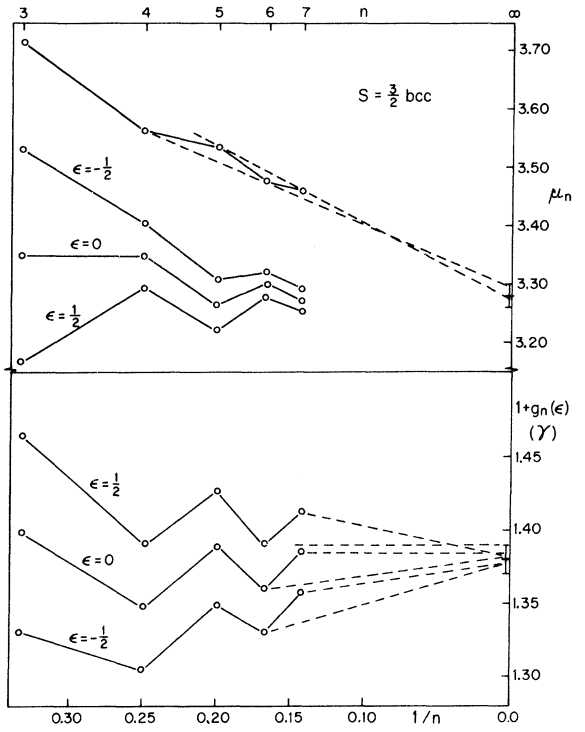

FIG. 1. Typical ratio plot for the susceptibility series showing (a) the ratios $\mu_n = a_n/a_{n-1}$ and the linear extrapolants of the ratios $\mu_n'(\epsilon) = \frac{1}{2}[(n+\epsilon)\mu_n - (n+\epsilon-2)\mu_{n-2}]$ plotted vs $1/n$, and (b) the extrapolants $g_n(\epsilon) = (n+\epsilon)[(\mu_n/\mu_\infty) - 1]$ for the exponent $\gamma - 1$. These plots are for the bcc, $S = \frac{3}{2}$ case: the value of μ_∞ taken as 3.280.

the spin-∞ model on the fcc lattices they find that Padé approximants to $[(d^2/dK^2)\ln\chi_0(K)]^{1/2}$ give seemingly excellent convergence to $\gamma = 1.375$ when using the series to eighth order. This value is also consistent with the evidence for the bcc and sc lattices. Unfortunately, on using the next two terms, this rapid convergence is seen to have been illusory, as shown in Table VI.[13(c)] (This Padé table should be compared with the one for the same case shown in Table IV, which supports the estimates quoted in Table V.) Bowers and Woolf also examined the spin-$\frac{1}{2}$ model with nearest- and next-nearest-neighbor model. Here they find $\gamma = 1.374$ for the fcc lattice using approximants to the logarithmic derivative. Again they find $\gamma = 1\frac{3}{8}$ to be consistent for the loose-packed lattices. However, their arguments are not really conclusive since they are based on a "self-consistent" method of finding the critical point corresponding to $\gamma = 1\frac{3}{8}$ and then estimating the exponent corresponding to this critical point. As is well known, there is a close correlation between the estimates of γ and K_c in most methods of extrapolation so that self-consistency is not a sufficient criterion of acceptability. [This correlation will be seen clearly if the data of Table IV are plotted as a graph of residues ($\simeq\gamma$) vs poles ($\simeq K_c$).]

It is evident from this short survey[13(c)] and an examination of Table V that the value of the exponent γ is not very well determined. On general grounds one expects γ to be independent of lattice structure; extensive experience with the Ising model (both exact and numerical results) confirms this.[2,3] Such an hypothesis is also borne out by the evidence of Table V. The question of the spin dependence is more problematical. Early work on the Ising model[18] suggested that the exponents were spin independent and this has been supported by recent further work for spin 1.[20] The longer series now available for spin ∞ tends to indicate[12(b)] $\gamma \simeq 1.23$, in place of $\gamma = 1.25$, but a more detailed analysis by Saul, Jasnow, and Wortis (see footnote 7 in Ref. 21) indicates that this is probably due to coincident (weaker) singularities masking the simple $\gamma = 1\frac{1}{4}$ behavior. The evidence for the Heisenberg model in Table V is equivocal. There is, without doubt, a general trend towards lower γ values with higher spin. This is most marked for the fcc data which might reasonably be represented by a formula such as $\gamma(S) \simeq 1.375 + [0.04/S(S+1)]$. For the loose-packed lattices, however, the trend is not as strong and there is even evidence for a *minimum* in $\gamma(S)$ around $S = \frac{5}{2}$; we cannot, however, take this seriously. Indeed, if we accept the lattice independence of γ and ignore the data for $S = \frac{1}{2}$, the uncertainties are really consistent with the hypothesis that $\gamma \simeq 1.38$ *independently of spin*. (See the row of weighted

TABLE IV. Sample Padé tables for the logarithmatic derivative of the susceptibility series showing roots (approximating K_c) and residues (approximating γ).

(A) bcc $S = \frac{3}{2}$

D \ N	1	2	3	4	5
1	0.27098	0.33329	0.28280	0.32519	0.28806
	1.015	1.889	0.979	1.969	0.951
2	0.29742	0.30427	0.30504	0.30480	
	1.277	1.368	1.382	1.376	
3	0.30487	0.30517	0.30486		
	1.379	1.385	1.378		
4	0.30516	0.30499		Estimates:	$K_c = 0.3049 \pm 2$
	1.385	1.381			$\gamma = 1.38 \pm 1$
5	0.30474				
	1.375				

(B) fcc $S = \infty$

D \ N	2	3	4	5	6	7
2	0.31442	0.31395	0.31418	0.31586	0.31501	0.31471
	1.364	1.351	1.358	1.481	1.402	1.381
3	0.31410	0.31408	0.31357	0.31506	0.31396	
	1.355	1.354	1.345	1.405	1.340	
4	0.31408	0.31409	0.31457	0.31471		
	1.354	1.355	1.373	1.381		
5	0.31364	0.31458	0.31474			
	1.346	1.374	1.383			
6	0.31537	0.31472		Estimates:	$K_c = 0.3147 \pm 3$	
	1.433	1.382			$\gamma = 1.38 \pm 2$	
7	0.31448					
	1.367					

TABLE V. Estimates of the exponent γ (the uncertainties are in the last place quoted).

Lattice \ S		$\frac{1}{2}$	1	$\frac{3}{2}$	$\frac{5}{2}$	∞
fcc	Padé	1.43±4	1.39±2	1.375±1	1.365±1	1.38±2
	Ratio	1.43±3	1.38±2	1.38±2	1.38±2	1.38±1
bcc	Padé	1.39±4	1.385±2	1.38±1	1.36±1	1.37±1
	Ratio	1.38±4	1.43±5	1.38±4	1.36±3	1.39±1
sc	Padé	1.42±2	1.39±7	1.38±4	1.365±4	1.38±2
	Ratio	?	1.43±3	1.41±2	1.39±2	1.37±1
Weighted average		1.415	1.392	1.381	1.367	1.378

mean estimates in Table V.) The series for $S=\frac{1}{2}$ seem definitely to support the large values reported,[11] but even though they are longer series they are certainly the most erratic and hardest to analyze. In view of Bowers and Woolf's analysis of the second-neighbor $S=\frac{1}{2}$ model[19] we are, in agreement with them, inclined to conclude that

$$\gamma = 1.375^{+0.02}_{-0.01} \tag{4.2}$$

is a good estimate for all spin (and all the cubic lattices). One may, however, leave open the possibility that γ is significantly higher just for $S=\frac{1}{2}$ and, in view of the relative shortness of the series, the uncertainties quoted in (4.2) may still be somewhat overly optimistic.[13(c)] Of course, the third decimal place in (4.2) has almost no significance: It merely represents the "conveniently close" fraction $1\frac{3}{8}$, which we will adopt for subsequent analyses. Since one of our main interests lies in the systematics with respect to spin and lattice structure, a somewhat higher working choice, such as 1.380 or 1.390, would not seriously affect our general conclusions.

Having accepted the estimate $\gamma \simeq 1\frac{3}{8}$, more reliable estimates of the critical point may be obtained by the standard ratio and Padé approximation methods. Typical results are shown in Fig. 2 and Table VII. The final estimates for the critical point K_c

TABLE VI. Padé table for $[(d^2/dK^2)\ln\chi_0(K)]^{1/2}$ for $S=\infty$ fcc (roots and residues).

D \ N	2	3	4	5	6
2	0.31446	0.31443	0.31443	0.31500	0.31485
	1.376	1.374	1.374	1.411	1.399
3	0.31443	0.31446	0.31458	0.31482	
	1.374	1.376	1.383	1.395	
4	0.31446	0.31482	0.31491		
	1.376	1.397	1.407		
5	0.31461	0.31491			
	1.383	1.407			
6	0.31482				
	1.397				

$= J/kT_c$ are collected in Table VIII and their dependence on spin and coordination number can be seen from Fig. 3. For "large" spin (actually $S \gtrsim 1$) the critical temperatures are well represented by

$$S^2 k_B T_c = \tfrac{1}{3} JS(S+1)(q-1)\,\theta_c[1 - e/S(S+1)], \tag{4.3}$$

with

$$\begin{aligned} &\theta_c = 0.8666, \quad e = 0.1296, \quad \text{fcc}(q=12), \\ &\theta_c = 0.8812, \quad e = 0.1587, \quad \text{bcc}(q=8), \\ &\theta_c = 0.8675, \quad e = 0.2011, \quad \text{sc}(q=6), \end{aligned} \tag{4.4}$$

where we may note that the mean-field approximation $T_c = T_0$ corresponds to $e \equiv 0$ and $\theta_c = q/(q-1)$. (See also Fig. 3.) Although the θ_c do not vary monotonically with q, the values of $(q-1)\theta_c/q = 0.795$, 0.771, and 0.723 (for $q=12$, 8, and 6, respectively) are monotonic.

The critical susceptibility amplitudes $A(K_c)$ were determined by forming Padé approximants to the series $A(K)$, defined via (4.1), and evaluating these at $K=K_c$. Any approximants with spurious poles in the region $|K| < K_c$ were discarded. The amplitudes A_c are presented in Table IX and Fig. 4. The mean-

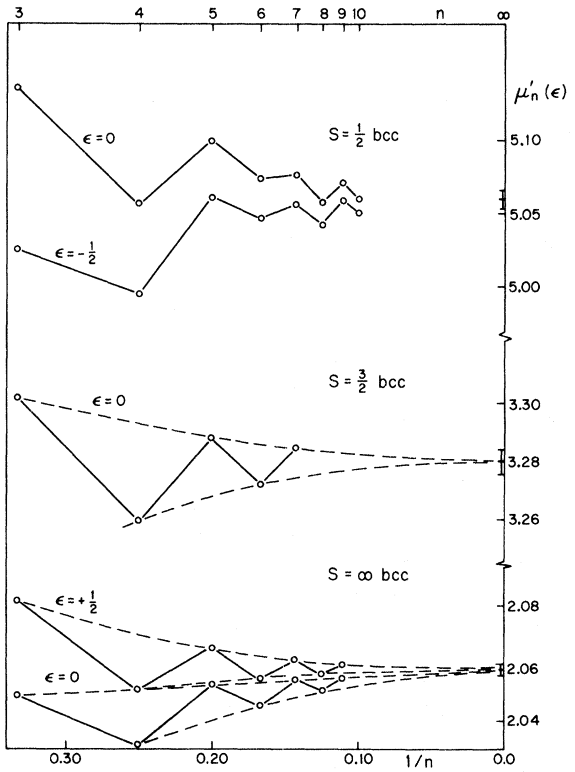

FIG. 2. Typical set of ratio plots to determine the critical point $k_B T_c/J$ from the susceptibility series given the value of the exponent γ as 1.375. The extrapolants $\mu^*_n(\epsilon) = (n+\epsilon)\mu_n/[(n+\epsilon)+(\gamma-1)]$ are plotted vs $1/n$ for the bcc lattice, with spin values $S=\frac{1}{2}$, $\frac{3}{2}$, and ∞.

TABLE VII. Sample Padé tables of $[\chi_0(K)]^{1/\gamma}$ with $\gamma = 1.375$ for the bcc lattice.

D \ N	2	3	4	5	6	7
2	0.19767	0.19726	0.19696	0.19728	0.19760	
3	0.19733	0.19646	0.19710	0.19667	0.19782	0.19771
4	0.19684	0.19714	0.19741	0.19732	0.19762	
5	0.19707	0.19768	0.19732	0.19738		
6	0.19641	0.19729	0.19744			
7	0.19776	0.19765				
	$K_c = 0.1974 \pm 0.0002$					
	$S = \frac{3}{2}$					
2	0.30482	0.30459	0.30476	0.30474		
3	0.30457	0.30469	0.30474			
4	0.30473	0.30474				
5	0.30474					
	$K_c = 0.30474 \pm 0.00004$					
	$S = \infty$					
3	0.48703	0.48691	0.48500	0.48651	0.48599	
4	0.48691	0.48708	0.48643	0.48638		
5	0.48618	0.48646	0.48637			
6	0.48650	0.48640				
7	0.48624					
	$K_c = 0.48638 \pm 0.0010$					

field prediction is

$$A_c^{\mathrm{mf}} = 1 . \tag{4.5}$$

Near the critical point we may write approximately

$$A(K) \simeq A_c[1 + a_1(1 - K/K_c)] , \tag{4.6}$$

where the constant a_1 may be determined from the Padé approximants. These estimates are presented in Table X, and are seen to change sign and increase monotonically with spin. Explicit "best" approximants for $A(K)$ and thence, through (4.1), for the susceptibility are given in Table XI.

B. Series for Correlation Moments

The tth moment of the correlation function is expected to diverge as a power law with an exponent $t\nu+\gamma$, that is,[2,3]

$$\mu_t(T) \sim [1 - (T_c/T)]^{-\gamma - t\nu} \quad (T \to T_c+) . \tag{4.7}$$

The second-moment series has been analyzed in detail for all the values of spin and for all three lattices. The values of K_c determined from the susceptibility series were used in forming estimates for the exponent from the ratios and in calculating Padé approximants to the series $(K - K_c)(d/dK)\ln\mu_2(K)$. As well as analyzing the second-moment series, we examined the series for $\mu_2(K)/\chi_0(K)$, which should diverge at K_c with an exponent 2ν. In addition, we constructed a "mean-square-size" series $\langle R_n^2 \rangle$ from the second-moment series by dividing the coefficients term by the corresponding susceptibility coefficients.[3] The mean-square-size function $R^2(K)$ must diverge at $K = 1$ and should have an exponent 2ν. In Fig. 5 and Table XII, we present representative examples of the ratio plots and Padé tables. The fourth-moment series was analyzed for the $S = \infty$ model in the same manner. However, the stronger divergence makes it a harder series to extrapolate reliably. Nevertheless it served to check the expectation (4.7) for $t = 4$ by yielding estimates for ν within ± 0.01 of those found from the second moments (see below). For $S = \infty$ the ratios and Padé approximants to μ_2/χ_0 appeared to give the smoothest and most precise results. For lower values of S the direct second-moment series yielded estimates with equal or less scatter. The mean-square-size series gave estimates for 2ν typically lower by 0.01–0.04 but the range of uncertainty was correspondingly larger and the estimates less consistent between the different lattices. The over-all weighted-average estimates for 2ν for each spin and lattice are listed in Table XIII. The uncertainties are again quite appreciable, especially for $S = \frac{1}{2}$. There appears to be a slight downward trend with spin; but there is also a tendency for the estimate of 2ν to increase as the coordination number falls. This lattice effect is almost certainly spurious: accepting that, we see that the evidence for any spin dependence is much weaker. In line with our assumptions for γ we will presume the value of ν to be independent of spin as well as of lattice structure. We are inclined to give a little more weight to the sc and bcc values relative to the fcc lattice whose high coordination number tends to give it a more mean-field-like behavior. (The tetrahedral lattice with $q = 4$ would presumably show the opposite effect.) Our final estimate is then

$$2\nu = 1.405^{+0.02}_{-0.01} , \tag{4.8}$$

where the asymmetric uncertainties allow for those in γ quoted in (4.2).[13(d)] However, it should be borne in mind that the uncertainties for the $S = \frac{1}{2}$ models considered alone would be much larger than indicated. In any case we have adopted the main value (4.8) (and $\gamma = 1\frac{3}{8}$) for all the subsequent calculations.

TABLE VIII. Estimates of the critical points $K_c = J/k_B T_c$ (the uncertainties are in the last place quoted).

Lattice \ S	$\frac{1}{2}$	1	$\frac{3}{2}$	$\frac{5}{2}$	∞
fcc	0.1241 ± 3	0.16795 ± 5	0.19558 ± 5	0.22815 ± 10	0.3147 ± 1
bcc	0.1974 ± 3	0.2632 ± 4	0.30474 ± 4	0.3543 ± 2	0.48635 ± 10
sc	0.2960 ± 3	0.383 ± 1	0.4385 ± 5	0.5060 ± 4	0.6916 ± 2

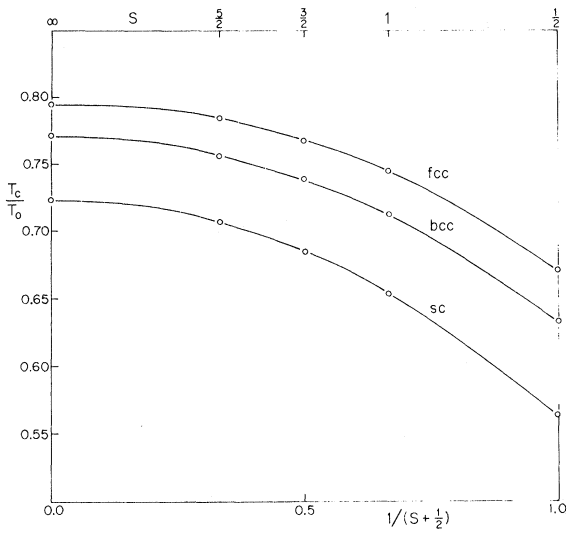

FIG. 3. Dependence of the critical temperature $k_B T_c/J$ on spin and lattice: a plot of T_c/T_0 vs $1/(S+\frac{1}{2})$, where T_0 is the mean-field critical temperature defined in Eq. (3.4).

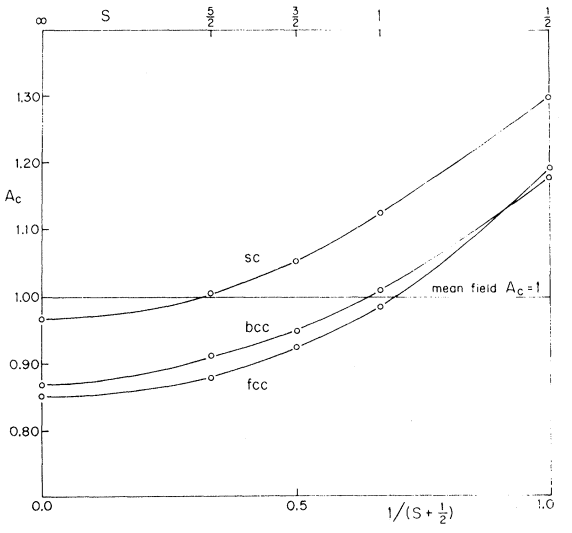

FIG. 4. Dependence of the critical susceptibility amplitude A_c on spin and lattice. The mean-field value for the amplitude is $A_c = 1$.

If we accept the basic exponent relation[2,3] $(2-\eta)\nu = \gamma$ and use $\gamma = 1\frac{3}{8}$, we find from (4.8) that

$$\eta = 0.043 \pm 0.014 \ . \tag{4.9}$$

It might be thought that the uncertainty in γ [see (4.2)], if taken into account, would lead to a significantly larger uncertainty in the value for η. This is actually not the case because of the correlation, already mentioned, between the estimates of γ and K_c. Thus an increase $\Delta\gamma$ in the assumed value of γ will, through the standard ratio analysis (on a $1/n$ plot) lead to an increase of about $\Delta K_c \simeq \Delta\gamma K_c/(n-1+\gamma)$ in the estimate of the inverse critical temperature from n terms of the susceptibility series. (This might be "amplified" by a factor of 2 or 3 through the extrapolation of the "trends" of successive estimates.) The increase ΔK_c, when used in the analysis of the μ_2 or μ_2/χ_0 series, will in turn lead to a *correlated* increase in the estimates of 2ν of

$$2\Delta\nu \simeq (n-1+2\nu)\Delta K_c/K_c \simeq \Delta\gamma(n-1+2\nu)/(n-1+\gamma) \ . \tag{4.10}$$

If η is calculated from $(2-\eta)\nu = \gamma$, the changes in γ and ν nearly cancel and one finds

$$\Delta\eta \simeq -\{(2\nu-\gamma)[1-(\gamma/n)]/2\nu^2\}\Delta\gamma \ . \tag{4.11}$$

With the values estimated for γ and ν the factor in braces lies between 0.05 and 0.09. Even with $\Delta\gamma = \pm 0.05$ this leads only to $\Delta\eta \simeq \mp 0.004$ or less, so that it is only the direct uncertainty in ν *given* γ that leads to the uncertainty in η. This is confirmed[13(d)] by a previous tentative analysis of the series for the fcc $S=\infty$ model[2(b),12(b)] based on $\gamma = 1.333$, which gave $\eta = 0.075 \pm 0.035$; this includes the present central estimate within its range of uncertainty even with no allowance for the change in assumed value of γ.

For mnemonic purposes it may be useful to represent the estimates for η by a simple fraction. From the many possibilities allowed by (4.9) the following alternatives seem the simplest which lie near the center of the range:

$$\eta = \tfrac{1}{24} \simeq 0.04167, \quad \gamma = 1\tfrac{3}{8}, \quad 2\nu = 1\tfrac{19}{47} \simeq 1.40425 \ , \tag{4.12}$$

and, which we prefer,

$$\eta = \tfrac{2}{45} \simeq 0.04444, \quad \gamma = 1\tfrac{3}{8}, \quad 2\nu = 1\tfrac{13}{32} = 1.40625 \ . \tag{4.13}$$

TABLE IX. Estimates for amplitude $A(K_c)$ (the uncertainties are in the last place quoted).

Lattice \ S	$\frac{1}{2}$	1	$\frac{3}{2}$	$\frac{5}{2}$	∞
fcc	1.190 ± 1	0.98476 ± 5	0.92456 ± 2	0.8797 ± 1	0.8520 ± 8
bcc	1.1770 ± 5	1.0092 ± 2	0.95020 ± 3	0.9114 ± 2	0.8686 ± 1
sc	1.2971 ± 2	1.124 ± 1	1.0518 ± 4	1.0040 ± 5	0.96647 ± 5

TABLE X. Estimates of the constant a_1 in Eq. (4.6).

Lattice \ S	$\frac{1}{2}$	1	$\frac{3}{2}$	$\frac{5}{2}$	∞
fcc	−0.27	0.011	0.08	0.19	0.23
bcc	−0.14	−0.05	0.07	0.13	0.24
sc	−0.17	−0.09	−0.02	0.03	0.07

(The simpler possibilities $\eta = \frac{1}{28} \simeq 0.0357$, $\gamma = 1\frac{3}{8}$, $2\nu = 1\frac{2}{5} = 1.400$ are also consistent with the error limits but lie rather close to one end of the range.) One might reasonably have adopted one of these sets of values for the rest of the numerical calculations but we have retained the estimate (4.8) for 2ν and used the nominal value $\eta = 2 - (\gamma/\nu) = 0.04270\ldots$ which then follows.

C. Exponent Relations

We note that the value of η for the Heisenberg models seems somewhat lower than for the three-dimensional Ising models ($\eta = 0.056 \pm 0.008 \simeq \frac{1}{18}$) although in view of the uncertainties this might not be significant. The values of γ and ν are, however, certainly different from the Ising values ($\gamma = 1.250$, $\nu \simeq 0.642$).

It is worth comparing the estimates for γ, η, and ν with those following from the familiar exponent or "scaling" relations which have been advanced on various grounds.[2] The so-called gap exponent Δ may be estimated from a study of the fourth and higher-field derivatives of the free energy. For spin $\frac{1}{2}$ these derivatives have been calculated by Baker *et al.*[10,11] but since they used $\gamma \simeq 1.43$ in their analysis we will not utilize their estimates. More recently, however, Stephenson and Wood[22(a)] have calculated and analyzed these series for $S = \infty$ on the fcc, bcc, and sc lattices. Their results may be stated as

$$\Delta - \gamma = 0.36 \pm 0.025 \,. \tag{4.14}$$

By the thermodynamic exponent relations $\Delta = \beta + \gamma$ this difference should equal β. In fact, by a special method due to Baker, these same authors[22(b)] have estimated β directly for the fcc lattice (only) finding

$$\beta = 0.38 \pm 0.03 \,. \tag{4.15}$$

Since their method effectively utilizes the magnetization curve only for $T < 0.99 T_c$ the agreement between (4.14) and (4.15) is quite satisfying. On accepting (4.14) the scaling relation $2 - \alpha = 2\beta + \gamma = 2\Delta - \gamma$ yields the prediction

$$2 - \alpha = 2.09 \pm 0.04 \quad \text{or} \quad \alpha = -0.09 \pm 0.04 \,, \tag{4.16}$$

where, as usual, the negative value of α indicates a finite, cusped specific-heat curve.[2] This value of α is not inconsistent with independent direct estimates (see also below) although these are not very precise. Thus for $S = \infty$ Jasnow and Wortis[12] estimated $\alpha \simeq -0.1$, while the analyses of Domb and

TABLE XI. Selected Padé approximants to $A(K)$. $A(K) \simeq (1 + p_1 K + \cdots + p_L K^L)/(1 + q_1 K + \cdots + q_M K^M)$.

	fcc		bcc		sc	
S	p_l	q_m	p_l	q_m	p_l	q_m
$\frac{1}{2}$	−7.4268	−8.3470	18.2015	17.1671	4.5963	3.2416
	27.3146	31.2128	11.9818	−4.6685	17.3070	13.8446
	−31.6562	−32.2152	314.3184	335.2731	38.8650	26.8813
	−34.4289	−80.3582	1837.5978	1446.4672	30.4452	11.9750
		−87.7438	769.4057	−208.3458	8.8253	
1	−1.6063	−1.4193	3.5178	3.4087	2.5774	2.1674
	−1.1913	−1.7676	1.4785	1.6914	6.1238	5.5048
	2.9002	2.0371	−0.61008	−0.46282	7.3166	5.4911
		−0.077721	1.4910			−0.61807
$\frac{3}{2}$	−3.8503	−3.4866	2.7906	2.8582	1.9766	1.7790
	5.0252	3.8863	0.28957	0.97004	0.92461	0.79561
	−5.2259	−4.2743	−0.96350	−0.35252	0.95267	1.0333
	1.2916		0.45440			
$\frac{5}{2}$	−3.3956	−2.9688	0.045613	0.19317	2.2423	2.1597
	0.41246	−0.58037	−2.7044	−2.2873	1.9675	1.9696
	2.0317	1.3062	1.6370	0.92326	0.77707	0.90043
	0.0010192					0.21954
∞	−4.9642	−4.5950	0.72952	0.89003	0.62369	0.61183
	8.1056	6.6160	−2.2907	−1.9209	−0.37657	−0.27988
	−2.8724	−1.1683	−0.83515	−1.0643	0.18076	0.21222
	−1.2990	−1.0599	0.87130	0.42039	0.13052	0.12206
	0.074558			0.068423		

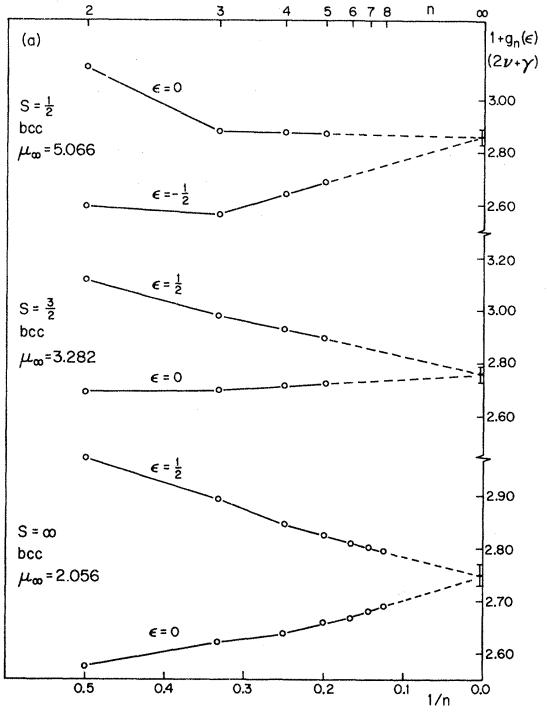

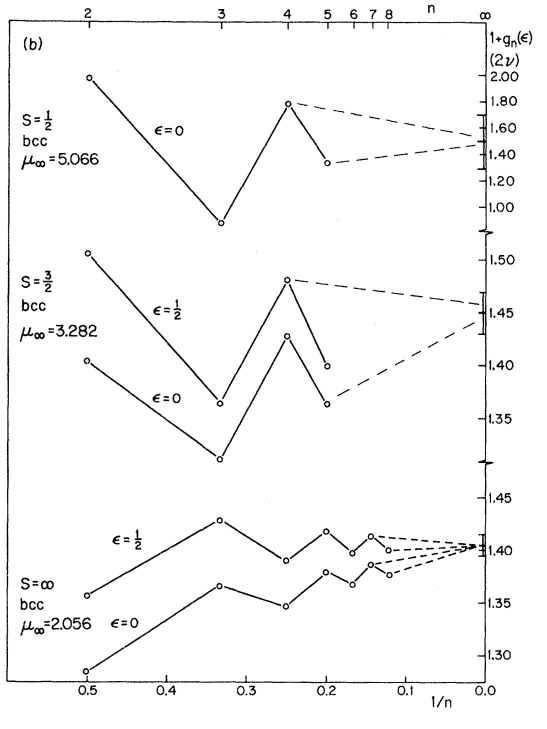

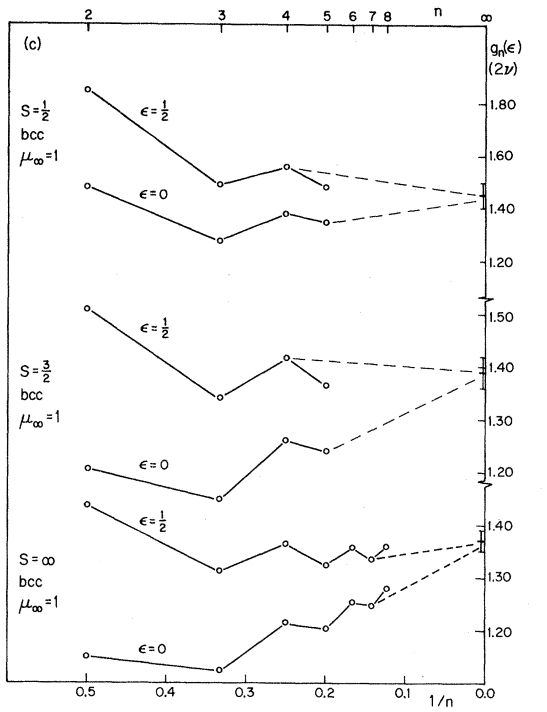

FIG. 5. Typical ratio plots for the correlation-length exponent ν using the extrapolants $g_n(\epsilon) = (n+\epsilon)(\mu_n/\mu_\infty - 1)$ for (a) the second moment $\mu_2(K)$; (b) the second moment divided by the susceptibility $\mu_2(K)/\chi_0(K)$; and (c) the second-moment series divided term by term by the susceptibility series $\langle R^2(K)\rangle$. Cases shown are for the bcc lattice, with spin values $S = \frac{1}{2}$, $\frac{3}{2}$, and ∞.

Bowers[23] and Stanley[24] may be summarized by

$$\alpha = -0.07 \pm 0.04 \,. \tag{4.17}$$

Bowers and Woolf[19] for the second-neighbor $S = \infty$ model concluded that $\alpha = -0.09 \pm 0.03$, which coincides with (4.16). On the other hand, for $S = \frac{1}{2}$ Baker *et al.*[11] estimated $\alpha \simeq -0.2$, although this was linked to their estimate $\gamma \simeq 1.43$. Finally, the thermodynamic scaling relation $\delta = 1 + (\gamma/\beta) = \Delta/(\Delta - \gamma)$ yields the prediction

$$\delta = 4.8 \pm 0.3 \,. \tag{4.18}$$

The estimate (4.15) with $\gamma = 1\frac{3}{8}$ gives $\delta \simeq 4.6$ but with a somewhat larger uncertainty.

Now we may test the dimension-dependent exponent relations[2(b),3] $d\nu = 2 - \alpha$ and $2 - \eta = d(\delta - 1)/(\delta + 1)$. By (4.17) the former gives

$$2\nu = 1.38 \pm 0.03 \,. \tag{4.19}$$

The central value here lies significantly below our direct estimate (4.8). This discrepancy is of the same sign and similar magnitude as in the three-dimensional Ising model[3] [where $2\nu \simeq 1.285$ while $\frac{2}{3}(2 - \alpha) \simeq 1.250$]. In this case, however, the uncertainties are sufficiently large that the deviation cannot really be considered significant. Indeed, if the indirect estimate (4.16) is used one finds $2\nu = 1.40 \pm 0.03$, which agrees well with the value accepted. The second d-dependent relation yields, with (4.18), the prediction $\eta = 0.035 \pm 0.055$. This again is slightly lower than our estimate although the uncertainty is sufficiently large to allow a zero (or

TABLE XII. Sample Padé tables for the exponent of the second-moment series (the values adopted for K_c are those given in Table VIII).

D \ N	$S=\frac{1}{2}$ bcc 1	2	3	D \ N	$S=\frac{3}{2}$ bcc 1	2	3	D \ N	$S=\infty$ bcc 2	3	4	5
					(a) $(K-K_c)D\ \ln\mu_2(K)\mid_{K=K_c}\simeq 2\nu+\gamma$							
1	3.08	2.53	3.52	1	2.71	2.72	2.78	2	2.755	2.762	2.782	2.771
2	2.65	2.79		2	2.72	2.60		3	2.762	2.746	2.772	
3	2.93			3	2.78			4	2.800	2.774		
								5	2.771			
	Estimates: 2.7 ± 0.2				2.7 ± 0.1					2.77 ± 0.03		
					(b) $(K-K_c)D\ \ln[\mu_2(K)/\chi_0(K)]\mid_{K=K_c}\simeq 2\nu$							
1	1.60	1.10	1.97	1	1.37	1.37	1.40	2	1.392	1.393	1.405	1.398
2	1.28	1.35		2	1.37	1.37		3	1.393	1.392	1.399	
3	1.38			3	1.40			4	1.418	1.399		
								5	1.398			
	Estimates: 1.4 ± 0.2				1.38 ± 0.02					1.40 ± 0.01		
					(c) $(K-K_c)D\ \ln\langle R_\eta^2\rangle\mid_{K=1}\simeq 2\nu$							
1	1.54	1.34	1.37	1	1.24	1.29	1.38	2	1.307	1.364	1.386	1.396
2	1.39	1.37		2	1.29	0.90		3	1.375	1.378	1.399	
3	1.37			3	1.39			4	1.379	1.372		
								5	1.403			
	Estimates: 1.37 ± 0.05				?					1.39 ± 0.01		

negative) value for η. [The value following from (4.15) and $\delta\simeq 4.6$ is $\eta\simeq 0.07$.] In any event, we must conclude that the evidence presently available is not in real conflict with the d-dependent scaling relations although there are some hints of a discrepancy similar to that in the Ising model.

D. Correlation Range

Numerical values for the inverse effective correlation range $\kappa_1(T)$ have been obtained by evaluating direct Padé approximants to the series for the function $f(K)$ defined by

$$(\kappa_1 a)^2 = 2dK^{-1} f(K)\ [1-(K/K_c)]^{2\nu} \quad (d=3)\ . \tag{4.20}$$

A set of "best" Padé approximants to $f(K)$ are listed in Table XIV. They can be used in (4.20) to reconstruct $\kappa_1(T)$ for all $T>T_c$. Near the critical point we can write

$$\kappa_1(T)a \simeq F_{1,c}[(T/T_c)-1]^{\nu}\{1-b_1[(T/T_c)-1]\}. \tag{4.21}$$

Estimates of the amplitudes $F_{1,c}$ and b_1 are listed in Tables XV and XVI, respectively. We note that the mean-field prediction is $(2d)^{1/2}=\sqrt{6}\simeq 2.449$. For $S\gtrsim 1\frac{1}{2}$ the values are well represented by the formula

$$F_{1,c}^{(q)}(S)\simeq F_{1,c}^{(q)}(\infty)[1-f^{(q)}/S(S+1)]\ , \tag{4.22}$$

where

$$f^{(q)}\simeq 0.2165,\ 0.2396,\ 0.2407\ ,$$

for $\tag{4.23}$

$$q=12\ (\text{fcc}),\ 8\ (\text{bcc}),\ 6\ (\text{sc})\ ,$$

respectively.

TABLE XIII. Estimates for the exponent 2ν (the uncertainties are in the last place quoted).

Lattice \ S	$\frac{1}{2}$	1	$\frac{3}{2}$	$\frac{5}{2}$	∞
fcc	1.40 ± 5	1.41 ± 2	1.39 ± 2	1.39 ± 2	1.39 ± 1
bcc	1.42 ± 7	1.41 ± 3	1.39 ± 2	1.40 ± 2	1.40 ± 1
sc	1.40 ± 5	1.42 ± 3	1.41 ± 2	1.41 ± 2	1.41 ± 2
Average	1.41	1.41_3	1.39_7	1.40	1.40

V. CORRELATION FUNCTION

To utilize the Fisher-Burford approximant for the total scattering, we must know the critical amplitude $\hat{D}$ of the correlation function, defined in (2.13) via

$$\hat{\Gamma}_c^{zz}(\vec{k})\approx\hat{\chi}_c(\vec{k})\approx\hat{D}/(ka)^{2-\eta}\ \text{ as }\ ka\to 0\ . \tag{5.1}$$

Equivalently, we must be able to calculate the amplitude D in the real-space expression

$$\Gamma_c^{zz}(\vec{r})\approx D/(r/a)^{d-2+\eta}\ \text{ as }\ r\to\infty\ . \tag{5.2}$$

By taking Fourier transforms the two amplitudes are easily seen to be related by

$$\hat{D}/D=4\pi\cos(\tfrac{1}{2}\pi\eta)\Gamma\ (1-\eta)(a^3/v_0)\ , \tag{5.3}$$

in three dimensions, where $\Gamma(z)$ is here the standard gamma function.

Fisher and Burford estimated the value of the amplitude D with the aid of the critical-point energy

TABLE XIV. Selected Padé approximants to $f(K)$. Note: We tabulate only p_0 to p_L and q_1 to q_M, $f(K) \simeq (p_0 + p_1 K + \cdots + p_L K^L)/(1 + q_1 K + \cdots + q_M K^M)$.

	fcc		bcc		sc	
S	p_l	q_m	p_l	q_m	p_l	q_m
$\frac{1}{2}$	0.08333	2.5579	0.12500	4.7346	0.16667	3.4277
	0.23995	29.3909	0.60651	20.6764	0.52905	16.0892
	1.0872	−15.3829	1.3877	−12.4890	1.2951	−10.0056
1	0.12500	1.3767	0.18750	2.5492	0.25000	1.9178
	0.24903	6.3909	0.52575	2.7314	0.45904	3.0770
	0.64273	−5.4996	0.40145	−2.8488	0.43604	−1.3308
$\frac{3}{2}$	0.15000	−0.47409	0.22500	1.5905	0.30000	1.2976
	0.02312	1.4991	0.42022	−0.17050	0.38384	1.0003
	0.14995	−3.3010	0.03107	−1.2897	0.19197	−0.64619
$\frac{5}{2}$	0.17857	−1.2436	0.26786	1.0688	0.35714	0.81664
	−0.11524	−1.4096	0.35920	−1.0473	0.29762	0.44060
	−0.29787	−0.090415	−0.13322	−0.41911	0.16053	−0.26101
∞	0.25000	−2.8904	0.37500	0.57829	0.50000	0.95149
	−0.60647	−1.3913	0.30018	−2.4228	0.49150	−0.52978
	−0.56098	9.2708	−0.75405	−0.70944	−0.20418	−0.063210
	1.9627	−5.7178	−0.38346	0.81549	0.001748	0.23040
	−0.74182		0.10682		0.10462	
	−0.039952					

U_c, which, by (3.8), is related directly to the nearest-neighbor correlation function by

$$\Gamma_c^{zz}(\vec{\delta}) = -2U_c/qJ(1+S^{-1}) \ . \tag{5.4}$$

In the two-dimensional Ising model the exact results may be written

$$D = \Gamma_c^{zz}(\vec{\delta})(1-\epsilon) \ , \tag{5.5}$$

where for the square lattice $\epsilon \simeq 0.00530$ while for the triangular lattice $\epsilon \simeq -0.00297$. By comparing the behavior of the function $(r/a)^{d-2+\eta}\Gamma_c^{zz}(\vec{r})$ (which should approach D as $r \to \infty$) for small values of $|\vec{r}|$ on the square and simple-cubic lattices Fisher and Burford concluded that (5.5) would probably hold in three dimensions if the magnitudes of ϵ were increased to 0.026 for the loose-packed sc and bcc lattices, and to $\epsilon = -0.016$ for the close-packed fcc lattice.

In this section we shall follow a similar procedure; in particular, we will first estimate U_c [or $\Gamma_c^{zz}(\vec{\delta})$] for all lattices and all spins, while for $S = \infty$ we will also estimate $\Gamma_c^{zz}(\vec{r})$ for small values of $\vec{r}$. [In addition, we have studied $\Gamma_c^{zz}(\vec{r})$ for the $S = \infty$ and $S = \frac{1}{2}$ cubic Ising models.] However, our subsequent estimate of the "correction" ϵ will be more soundly based since we have examined carefully the full Fourier inversion involved and the characteristic way the lattice structure enters. We will see, in fact, that Fisher and Burford probably underestimated the magnitude of ϵ by a significant amount (although none of their general conclusions are altered).

TABLE XV. Estimates of the amplitude of the correlation function F_{1c}.

Lattice \ S	$\frac{1}{2}$	1	$\frac{3}{2}$	$\frac{5}{2}$	∞
fcc	1.90 ± 2	2.185 ± 5	2.288 ± 2	2.366 ± 2	2.427 ± 7
bcc	1.85 ± 5	2.111 ± 5	2.212 ± 2	2.283 ± 2	2.364 ± 2
sc	1.67 ± 4	1.906 ± 7	2.013 ± 2	2.089 ± 2	2.152 ± 2

A. Extrapolation of Correlation Functions

In order to extrapolate the correlation functions reliably to $T = T_c$ it is essential to allow for their singularities at the critical point. We shall assume that the nature of the leading temperature singularity in $\Gamma^{zz}(\vec{r}; T)$ is the same for all $\vec{r}$. This is known to be rigorously true for the soluble two-dimensional Ising models and there are strong arguments for its general validity.[2,3] Since the nearest-neighbor correlation function is proportional to the energy $U(T)$ we hence have

$$\Gamma^{zz}(\vec{r}; T) \approx \Gamma_c^{zz}(\vec{r}) - E(\vec{r})[1-(K/K_c)]^{1-\alpha} + B(\vec{r})[1-(K/K_c)] + \cdots \tag{5.6}$$

as $K = J/k_B T_c \to K_c$, where the second term is nonsingular at K_c but may nonetheless dominate the first term if the specific-heat exponent α is negative.

In fact, as mentioned in Sec. IV C, one may estimate α through the scaling relations using the estimates for ν and γ, with the result $\alpha \simeq -0.10$ [see Eq. (4.16)]. We have checked this by a direct analysis of the series for $S \geq 1$, although only the

TABLE XVI. Estimates of parameter b_1, defined by Eq. (4.21).

Lattice \ S	$\frac{1}{2}$	1	$\frac{3}{2}$	$\frac{5}{2}$	∞
fcc	0.12	0.23	0.28	0.33	0.38
scc	0.16	0.23	0.27	0.30	0.37
sc	0.15	0.18	0.21	0.23	0.25

series for $S=\infty$ lead to more precise estimates. Indeed, as noted before, Domb and Bowers[23] and Stanley[24] concluded that $\alpha \simeq -0.07$ for $S=\infty$. For $S=\frac{1}{2}$ Baker *et al.*[11] estimated $\alpha \simeq -0.2$ but we shall not give this weight here since it was based on a critical point consistent with $\gamma \simeq 1.43$. In summary, we shall adopt

$$\alpha \simeq -0.10 \tag{5.7}$$

for the purpose of extrapolating the $\Gamma^{zz}(\vec{r})$ to $T=T_c$. Fortunately, the numerical results are fairly insensitive to the precise value of α.

The values of $\Gamma_c^{zz}(\vec{r})$ were found by extrapolating the partial sums

$$S_N(\vec{r}) = \sum_{n=1}^{N} q_n(\vec{r}) K_c^n \tag{5.8}$$

[see (3.6)] to $N=\infty$ using the accepted estimates for K_c. The relation (5.6) implies that the term $q_n(\vec{r})K_c^n$ decreases asymptotically like $n^{-(2-\alpha)}$ so that the partial sums $S_N(\vec{r})$ should approach their limit $S_\infty(\vec{r})$ linearly with $N^{-(1-\alpha)}$ for large N. The extrapolation may be made roughly on a plot vs $N^{-1+\alpha}$ but to take systematic account of the noticeable curvature of these plots Neville tables were constructed to effect the extrapolation.[25] This method effectively fits polynomials of successively higher order (in the chosen variable) to the partial sums: The explicit formula used in pth order is

$$\Sigma_N^{(p)} = \frac{N^{1-\alpha}\Sigma^{(p-1)} - (N-p)^{1-\alpha}\Sigma_{N-1}^{(p-1)}}{N^{1-\alpha} - (N-p)^{1-\alpha}} \quad . \tag{5.9}$$

The results of these procedures are presented in Tables XVII and XVIII. As explained, the values of $\Gamma_c^{zz}(\vec{\delta})$ are proportional to the critical energy U_c [see (5.4)]. For $S \gtrsim 1\frac{1}{2}$ the following formula represents our results:

$$\Gamma_c^{(S,q)}(\vec{\delta}) \simeq \Gamma_c^{(\infty,q)}(\vec{\delta})[1 - u^q/S(S+1)] \, , \tag{5.10}$$

with

$$u^{(q)} \simeq 0.173, \quad 0.254, \quad 0.411$$

for $\tag{5.11}$

$$q = 12 \text{ (fcc)}, \quad 8 \text{ (bcc)}, \quad 6 \text{ (sc)}, \quad \text{respectively.}$$

We may mention that we also examined direct Padé approximants to the energy series. These give results systematically 5% lower than those quoted in Table XVII: We discount this, however, since the direct approximants are known to be poor when the energy is nearly cusplike as implied by $\alpha \simeq 0$.

TABLE XVII. The critical value of the nearest-neighbor correlation function (uncertainties are in the last place).

Lattice \ S	$\frac{1}{2}$	1	$\frac{3}{2}$	$\frac{5}{2}$	∞
fcc	0.187 ± 5	0.224 ± 2	0.235 ± 2	0.242 ± 2	0.2468 ± 5
bcc	0.199 ± 6	0.240 ± 3	0.254 ± 3	0.263 ± 3	0.273 ± 2
sc	0.222 ± 9	0.268 ± 5	0.295 ± 5	0.312 ± 5	0.329 ± 2

In Figs. 6(a)-6(c) the results for $\Gamma^{zz}(\vec{r})$ are displayed for the sc, bcc, and fcc lattices, respectively, by plotting

$$\mathfrak{D}(\vec{r}) = (r/a)^{1+\eta}\Gamma_c^{zz}(\vec{r})/\Gamma_c^{zz}(\vec{\delta}) \tag{5.12}$$

against r. Note that data are shown for $S=\infty$ Heisenberg and $S=\frac{1}{2}$ and ∞ Ising models (although these are not tabulated). By (5.2) and (5.5) we expect $\mathfrak{D}(r)$ to approach an asymptotic value of $(1-\epsilon)$ as $r \to \infty$. Evidently, the complete asymptotic region has not been reached by $r \simeq 3a$, which is the greatest distance for which the partial sums can be extrapolated with reasonable confidence. However, in view of the relative uncertainties indicated at the bottom of the plots, the variation might well be within 6 or 7% of an asymptotic limit. The most striking fea-

TABLE XVIII. The critical values of the correlation function (uncertainties are in the last place).

Lattice	$\vec{r}$	$S=\infty$ Heis	$S=\infty$ Ising	$S=\frac{1}{2}$ Ising
fcc	(1, 1, 0)	0.2468 ± 5	0.2776 ± 5	0.2475 ± 5
	(2, 0, 0)	0.1624 ± 5	0.183 ± 1	0.163 ± 1
	(2, 1, 1)	0.1375 ± 10	0.155 ± 1	0.138 ± 1
	(2, 2, 0)	0.120 ± 1	0.135 ± 1	0.120 ± 2
	(3, 1, 0)	0.105 ± 1	0.118 ± 2	0.105 ± 2
	(2, 2, 2)	0.098 ± 1	0.108 ± 2	0.097 ± 2
	(3, 2, 1)	0.090 ± 3	0.102 ± 3	0.090 ± 3
	(3, 3, 0)	0.080 ± 3	0.091 ± 3	0.080 ± 4
bcc	$\frac{1}{2}$(1, 1, 1)	0.273 ± 2	0.3106 ± 7	0.2735 ± 7
	(1, 0, 0)	0.199 ± 2	0.228 ± 2	0.200 ± 2
	(1, 1, 0)	0.156 ± 2	0.179 ± 2	0.157 ± 2
	(1, 1, 1)	0.131 ± 3	0.149 ± 2	0.131 ± 3
	$\frac{1}{2}$(3, 1, 1)	0.130 ± 3	0.146 ± 3	0.129 ± 3
	$\frac{1}{2}$(3, 3, 1)	0.104 ± 6	0.117 ± 4	0.101 ± 5
	$\frac{1}{2}$(3, 3, 3)	0.088 ± 6	0.102 ± 7	0.085 ± 5
sc	(1, 0, 0)	0.329 ± 2	0.387 ± 2	0.332 ± 1
	(1, 1, 0)	0.206 ± 2	0.245 ± 2	0.208 ± 2
	(2, 0, 0)	0.159 ± 2	0.190 ± 2	0.162 ± 4
	(1, 1, 1)	0.161 ± 5	0.194 ± 4	0.164 ± 4
	(2, 1, 0)	0.134 ± 5	0.160 ± 4	0.135 ± 7
	(3, 0, 0)	0.108 ± 12	0.126 ± 8	0.104 ± 7
	(2, 1, 1)			0.120 ± 7
	(2, 2, 0)			0.104 ± 7
	(3, 1, 0)			0.095 ± 7
	(4, 0, 0)			0.080 ± 9

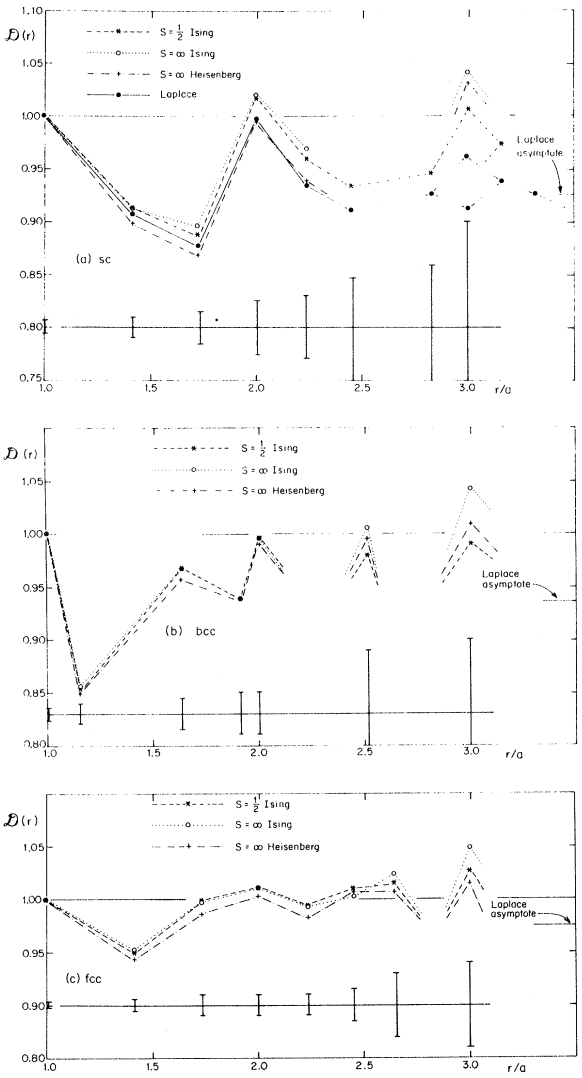

FIG. 6. Short-range behavior of the correlation function at the critical point as revealed by $\mathfrak{D}(\vec{r}) = (r/a)^{1+\eta}\Gamma_c^{zz}(\vec{r})/\Gamma_c(\vec{\delta})$ vs r/a for the $S=\frac{1}{2}$ and $S=\infty$ Ising models and the $S=\infty$ Heisenberg models on (a) the sc lattice; (b) the bcc lattice, and (c) the fcc lattice. In addition, the Green's function $\mathcal{G}_0(r)$ for the discrete Laplace equation is shown for the sc lattice and the asymptotic value of $\mathcal{G}_0(r)/(r/a)$ is indicated for all the lattices. The uncertainties of extrapolation are indicated by the "error bars" shown below the main plots. Missing values represent positions for which the correlation series could not be summed with acceptable accuracy.

ture of these graphs is that the values for all three distinct spin models are almost coincident for each separate lattice. Indeed, the differences between them lie *within* the apparent numerical uncertainties. On the other hand, the pattern of oscillation of each lattice is quite distinctive. This indicates the overwhelming importance of the lattice geometry for the relative variation of the correlation functions at short distances. We now examine this point more closely.

B. Lattice Green's Functions

Consider Laplace's equation $\nabla^2 v = 0$ on a discrete lattice space; it can be written

$$\sum_{\vec{\delta}} [v(\vec{r}) - v(\vec{r}+\vec{\delta})] = 0 , \tag{5.13}$$

the sum running over the nearest-neighbor vectors $\vec{\delta}$. The Green's function $\mathcal{G}_0(\vec{r})$ for this equation is defined by the solution of (5.13) with the inhomogeneous term

$$\delta_{\vec{r},\vec{0}} = 1 \text{ if } \vec{r} = \vec{0}$$
$$= 0 \text{ otherwise,} \tag{5.14}$$

on the right-hand side under the boundary condition $\mathcal{G}_0(\vec{r}) \to 0$ as $r \to \infty$. By taking Fourier transforms we find immediately

$$\hat{\mathcal{G}}_0(\vec{k}) = 1/[\textstyle\sum_{\vec{\delta}}(1 - e^{i\vec{k}\cdot\vec{\delta}})]$$
$$= 2d/qa^2\hat{K}^2(\vec{k}) , \tag{5.15}$$

where the effective wave number $\hat{K}(\vec{k}) = k[1 + O(k^2a^2)]$ was defined in (2.17). We now recognize [either from (5.15) or (5.13)] that $\mathcal{G}_0(\vec{r})$ is just proportional to the mean-field (or Ornstein-Zernike) approximation[3] for the correlation function *at* the critical point [$\kappa_1 \equiv 0$]. The observation that the details of the model seem inessential to the relative behavior of the correlations at small $\vec{r}$ suggests that the variation of $\mathcal{G}_0(\vec{r})$ in the same region should provide a good "mimic."

We can test this by inverting the solution (5.14). For the simple-cubic lattice with $\vec{r} = (la, ma, na)$ this yields the well-known integral

$$\mathcal{G}_0(l, m, n)$$
$$= (2\pi)^{-3}\int_{-\pi}^{\pi}\int_{-\pi}^{\pi}\int_{-\pi}^{\pi} \frac{\cos l\theta_1 \cos m\theta_2 \cos n\theta_3 \, d\theta_1 \, d\theta_2 d\theta_3}{2(3 - \cos\theta_1 - \cos\theta_2 - \cos\theta_3)} , \tag{5.16}$$

which has been extensively tabulated.[26] To make a comparison with the variation of $\Gamma_c^{zz}(\vec{r})$ we have plotted the reduced Green's function $(r/a)\mathcal{G}_0(\vec{r})/\mathcal{G}_0(\vec{\delta})$ on Fig. 6(a) on the same scale as the reduced correlation function $\mathfrak{D}(\vec{r})$. The general nature of the behavior is remarkably similar: All plots indicate the enhanced correlation along the lattice axes, i.e., at the integral points $r = na$ ($n = 1, 2, 3, \ldots$), and depressed correlations at the minima of the function

$$\sigma(\vec{r}) = |\vec{r}|/s(\vec{r})$$
$$= (l^2 + m^2 + n^2)^{1/2}/(|l| + |m| + |n|) , \quad \text{(sc)} \tag{5.17}$$

which is simply the ratio of the geometrical distance $|\vec{r}|$ to the lattice graph distance $s(\vec{r})$. Indeed, the peaks and troughs of $\sigma(\vec{r})$ correspond precisely to

those of the reduced Green's function and of $\mathfrak{D}(\vec{r})$, as can be seen in Fig. 7. This figure also shows $\sigma(\vec{r})$ for the bcc and fcc lattices where it again matches the behavior of $\mathfrak{D}(\vec{r})$. The closeness of the central estimates of $\mathfrak{D}(\vec{r})$ to the Green's function and their systematic variation suggests that the accuracy may be rather better than indicated by the quoted uncertainty limits.

Whereas we do now know the asymptotic value of $\mathfrak{D}(\vec{r})$ we can easily compute the exact limiting amplitude for the Green's function $\mathcal{G}_0(\vec{r})$; it is marked on the graph in Fig. 6(a). However, this function has an asymptotic decay corresponding to $\eta = 0$, whereas the approximant to be used for the scattering has the form

$$\hat{\mathcal{G}}_\eta(\vec{k}) \propto [\hat{K}(\vec{k})]^{-(2-\eta)} \tag{5.18}$$

with $\eta > 0$. To judge the significance of this we perform the inversion for the sc lattice to obtain

$$\mathcal{G}_\eta(\vec{r}) = (2\pi)^{-3}\int_{-\pi}^{\pi}\int_{-\pi}^{\pi}\int_{-\pi}^{\pi} \frac{\cos l\theta_1 \cos m\theta_2 \cos n\theta_3 \, d\theta_1 \, d\theta_2 \, d\theta_3}{[2(3-\cos\theta_1-\cos\theta_2-\cos\theta_3)]^{1-\eta/2}}. \tag{5.19}$$

The standard reduction developed by Montroll[26] may now be employed: The denominator is rewritten using the gamma function identity

$$\Gamma(\zeta) z^{-\zeta} = \int_0^\infty e^{-zt} t^{\zeta-1} \, dt \tag{5.20}$$

and the definition

$$I_n(x) = \pi^{-1}\int_0^\pi e^{x\cos\theta} \cos n\theta \, d\theta \tag{5.21}$$

of the Bessel function of imaginary argument is utilized to yield

$$\mathcal{G}_\eta(\vec{r}) = [\Gamma(1-\tfrac{1}{2}\eta)]^{-1}\int_0^\infty I_l(t) I_m(t) I_n(t) e^{-3t} t^{\eta/2} dt \, . \tag{5.22}$$

This integral has been evaluated numerically using Simpson's rule over a finite range, and an asymptotic expansion for large argument, over the remaining interval. The reduced Green's function $(r/a)^{1+\eta}\mathcal{G}_\eta(\vec{r})/\mathcal{G}_\eta(\vec{\delta})$ is displayed in Fig. 8 for $\eta = 0$ (as before) and $\eta = 0.0427$. The two plots are very close, as are the asymptotic values $(1-\epsilon_\eta) = 0.925$ and 0.923, respectively. We have examined $\mathcal{G}_\eta(\vec{r})$ only for the sc lattice, since the corresponding integrals are more awkward to compute for the bcc and fcc lattices. However, since η is rather small we expect the reductions in relative asymptotic amplitudes for the bcc and fcc to be quite similar (i.e., about 0.2%). To within the precision of the numerical extrapolations for these lattices, we may therefore take the relative amplitudes from the $\eta = 0$ case. (Note again in Fig. 6 that the differences between the various plots lie *within* the uncertainty limits.) The tables of Mannari and Kawabata[27] give $\mathcal{G}_0(\vec{0})$ for all three lattices. Use of the defining recurrence relation

$$q\mathcal{G}_0(\vec{0}) - \sum_{\vec{\delta}} \mathcal{G}_0(\vec{\delta}) = 1 \tag{5.23}$$

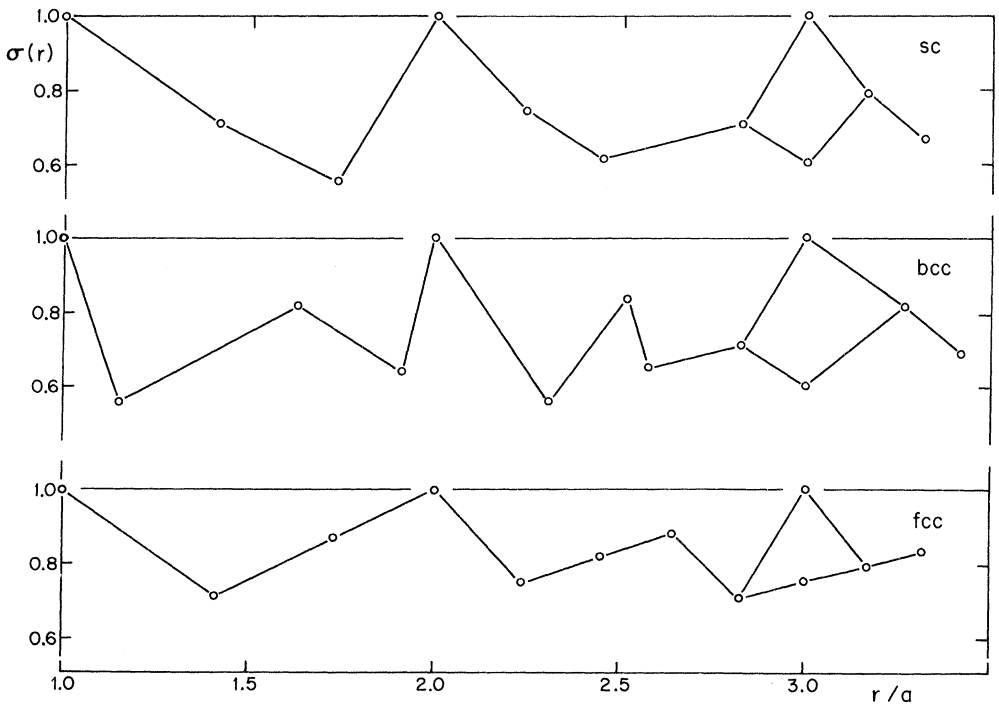

FIG. 7. Dependence of the function $\sigma(\vec{r}) = |\vec{r}|/s(r)$ on distance (r/a) for the sc, bcc, and fcc lattices. Note that the maxima and minima correspond exactly with those of the correlation function shown in Fig. 6.

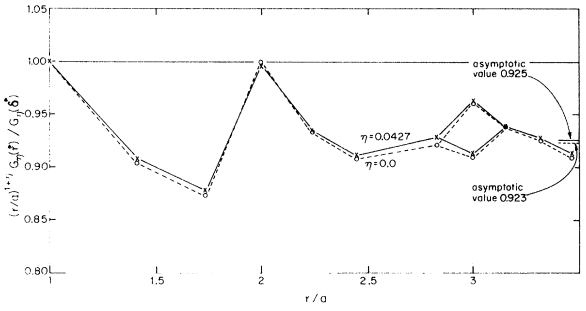

FIG. 8. Short-range behavior of $(r/a)^{1+\eta}\mathcal{G}_\eta(\vec{r})/\mathcal{G}_\eta(\vec{\delta})$ for $\eta=0$ and $\eta=0.0427$. Note that the two curves almost coincide and, in particular, their asymptotic values are closely similar.

[see (5.13) and (5.14)] then yields $\mathcal{G}_0(\vec{\delta})$ which, by symmetry, is independent of $\vec{\delta}$. Table XIX lists these $\eta=0$ data and the corresponding estimates of the reduction ϵ. The reductions correspond to 2.0, 6.5, and 7.5% for the fcc, bcc, and sc lattices, respectively. (For application these values could well be increased by 0.2% to allow for the nonzero value of η but, as mentioned, the available precision and knowledge hardly justifies this.) The corresponding estimates of Fisher and Burford hence appear to have been too small by differences of 3.6, 3.9, and 4.9%, respectively. (The corresponding changes in their numerical work will be mentioned below.) From the values of ϵ we can, via (5.5), Table XVII, and (5.3) estimate the amplitudes D and $\hat{D}$ [see (5.1) and (5.2)]. Our estimates for $\hat{D}$ are listed in Table XXI, which also contains the revised estimates for the $S=\frac{1}{2}$ Ising model.

Finally, Fig. 9 is a direct plot of $(r/a)\Gamma_c^{zz}(\vec{r})/\Gamma_c^{zz}(\vec{\delta})$ for the Ising and Heisenberg models; for reference $(r/a)\mathcal{G}_0(\vec{r})/\mathcal{G}_0(\vec{\delta})$ is also shown. For all three models the plots of the correlation functions drop increasingly below the $\eta=0$ Green's function. This is a direct (although not very precise) indication that $\eta>0$ for these three-dimensional models.

VI. SCATTERING APPROXIMANTS

We are now in a position to calculate the scattering curves using the Fisher-Burford approximant (2.16). This may be conveniently rewritten as

$$\hat{\chi}(\vec{k},T)\simeq\left(\frac{a}{r_1}\right)^{2-\eta}\frac{[(\kappa_1 a)^2+\phi^2 a^2\hat{K}^2(\vec{k})]^{\eta/2}}{(\kappa_1 a)^2+\psi a^2\hat{K}^2(\vec{k})}, \quad (6.1)$$

where the "effective interaction range" $r_1(T)$ is defined through

$$\chi_0(T)=[r_1(T)\kappa_1(T)]^{-(2-\eta)}. \quad (6.2)$$

The form (6.1) has the advantage that the prefactor $(a/r_1)^{2-\eta}$ remains finite at the critical point.

To estimate $r_1(T)$ via (6.2) one may form its series expansion and examine direct Padé approximants [since $r_1(T)$ is expected to be at most weakly singular at T_c]. However, these approximants are found to be rather poorly convergent at the critical point, although they do verify the amplitude consistency relation

$$(r_1/a)_c F_{1c}(A_c)^{1/(2-\eta)}=1 \quad (6.3)$$

to within 1% [see (4.1) and (4.21)]. As a numerically more satisfactory alternative to the use of direct approximants to the $r_1(T)$ series, we have employed the best approximants for $A(K)$ and $f(K)$ [see (4.1) and (4.21)] already listed in Tables XI and XIV, and calculated $r_1(T)$ from

$$(a/r_1)^{2-\eta}=[2df(K)/K]^{1-\eta/2}A(K) \quad (\text{with } d=3). \quad (6.4)$$

This procedure, of course, guarantees (6.3) and was found to be very satisfactory. Near the critical point one finds

$$r_1(T)/a=(r_1/a)_c\{1-c[(T/T_c)-1]+\cdots\}, \quad (6.5)$$

where the values of $(r_1/a)_c$, c, and $(a/r_1)_c^{2-\eta}$ are listed in Table XX. It is interesting to compare these values with those for the $S=\frac{1}{2}$ Ising model where $(r_1/a)_c$ varied from 0.440 to 0.464 and c from 0.457 to 0.491 as q went from 12 to 6.[3]

We have not derived any series for the true correlation range $\kappa(T)$ [defined by $\Gamma^{zz}(\vec{r})\sim e^{-\kappa r}$ as $r\to\infty$ for $T>T_c$], as did Fisher and Burford for the sim-

TABLE XIX. Estimates for the parameter ϵ [see Eqs. (5.1)–(5.5) and subsequent text]. Note that $D_0=\lim_{r\to\infty}(r/a)\mathcal{G}_0(\vec{r})$.

Lattice	$q\mathcal{G}_0(\vec{\delta})$	qD_0	ϵ
fcc	0.344 661	0.337 614	0.020
bcc	0.393 204	0.367 553	0.065
sc	0.516 386	0.477 465	0.075

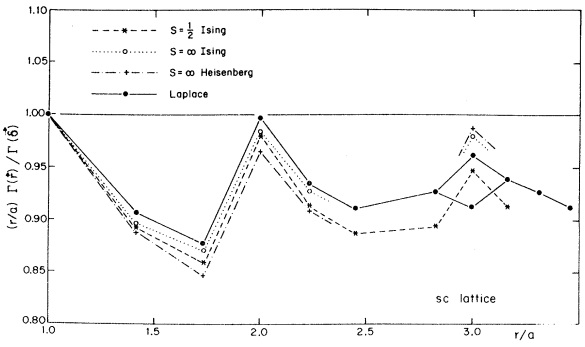

FIG. 9. Variation of $(r/a)\Gamma_c(\vec{r})/\Gamma_c(\vec{\delta})$ with distance for the sc lattice for the three models: $S=\frac{1}{2}$ Ising, $S=\infty$ Ising, and $S=\infty$ Heisenberg. In addition, $(r/a)\mathcal{G}_0(\vec{r})/\mathcal{G}_0(\vec{\delta})$ is plotted. Note that the curves for the three models fall beneath that for Green's function. This is evidence that $\eta>0$.

TABLE XX. The critical-point parameters for $r_1(T)$.

Spin	Lattice	$(a/r_1)_c^{2-\eta}$	$(r_1/a)_c$	c
$\frac{1}{2}$	fcc	4.17	0.482	0.43
	bcc	3.94	0.496	0.46
	sc	3.55	0.523	0.45
1	fcc	4.543	0.462	0.46
	bcc	4.359	0.471	0.46
	sc	3.971	0.494	0.47
$\frac{3}{2}$	fcc	4.668	0.455	0.45
	bcc	4.494	0.464	0.46
	sc	4.139	0.484	0.47
$\frac{5}{2}$	fcc	4.752	0.451	0.46
	bcc	4.589	0.459	0.45
	sc	4.243	0.478	0.47
∞	fcc	4.833	0.447	0.44
	bcc	4.679	0.455	0.44
	sc	4.331	0.473	0.47

ple-cubic $S=\frac{1}{2}$ Ising model.[3] Accordingly, we cannot form any high-temperature series for $\phi(T)$ and $\psi(T)$. Following the arguments of Fisher and Burford for the bcc and fcc Ising lattices, however, we satisfy ourselves by setting

$$\phi(T)=\phi_c(K/K_c)^3=\phi_c(T_c/T)^3 , \tag{6.6}$$

where ϕ_c is chosen to yield the correct critical-point decay amplitude $\hat{D}$ determined in Sec. V. In fact, one finds that little is lost except at high temperatures if $\phi(T)$ is merely set equal to ϕ_c. Note by (2.18) that $\psi(T)$ is always fixed from

$$\psi(T)=1+\tfrac{1}{2}\eta\phi^2(T) . \tag{6.7}$$

Last, the equation determining ϕ_c is

$$\phi_c^{\eta}=\hat{D}(r_1/a)_c^{2-\eta}(1+\tfrac{1}{2}\eta\phi_c^2) ; \tag{6.8}$$

this has been solved numerically by the Newton-Raphson method with the results shown in Table XXI. This table also lists the revised estimates for the $S=\frac{1}{2}$ Ising models.

Summary

To summarize the outcome of our numerical work: The *reduced scattering intensity* $\hat{\chi}(\vec{k}, T)$, defined in (2.7), for wave number $\vec{k}$ and temperature $T=(J/k_BK)\geq T_c$, can be calculated for the fcc, bcc, and sc lattices, and general spin (specifically: $S=\frac{1}{2}$, 1, $\frac{3}{2}$, $\frac{5}{2}$, and ∞), from Eq. (6.1) in which (i) the nearest-neighbor *lattice spacing* is a; (ii) the *effective interaction range* $r_1(T)$ is determined by (6.4) using Tables XI and XIV or, in the critical region, from Table XX; (iii) the *inverse correlation length* $\kappa_1(T)$ is given by (4.20) with $2\nu=1.405$ and using Table XIV or, in the critical region, Eq. (4.21) and Tables XV and XVI; (iv) the *exponent* $\eta\simeq 0.0427$ is determined by $(2-\eta)\nu=\gamma=1.375$; (v) the *effective wave vector* $\hat{K}(\vec{k})$ is defined by (2.17); (vi) the *critical shape functions* $\phi(T)$ and $\psi(T)$ are given by (6.6) and (6.7) with Table XXI.

We recall, in addition, that values of the critical-point spin-spin correlation functions $\Gamma_c^{zz}(\vec{r})$, defined in (2.3) and (2.6), are listed in Tables XVII and XVIII (see also Fig. 6). From these, via (3.8), follow the values of the critical-point energy. Estimates for the specific-heat exponent α and other exponents are reviewed in Sec. IV C.

VII. DISCUSSION

Using the work summarized at the end of Sec. VI we now review the graphical and numerical predictions for the critical scattering.

A. Universality

In the critical region the approximant (6.1) assumes the scaling form[2]

$$\hat{\chi}(\vec{k}, T)\approx\hat{\mathfrak{D}}(\kappa_1/k)/(ka)^{2-\eta} , \tag{7.1}$$

with $\kappa_1(T)\cong F_{1c}(\Delta T/T_c)^{\nu}$ and the scaling function

$$\hat{\mathfrak{D}}(y)=\hat{D}\frac{[1+(y/\phi_c)^2]^{\eta/2}}{1+y^2(1+\frac{1}{2}\eta\phi_c^2)^{-1}} , \tag{7.2}$$

which, when $y\to\infty$, varies as

$$\hat{\mathfrak{D}}(y)\approx\hat{D}_\infty y^{-(2-\eta)}[1-y^{-2}+\cdots] , \tag{7.3}$$

with $\hat{D}_\infty=(1+\frac{1}{2}\eta\phi_c^2)\phi_c^{-\eta}\hat{D}$. We have noted (in Sec. IV B) that the exponents η and ν are apparently independent of lattice and spin and are hence "universal" for the three-dimensional isotropic Heisenberg models. However, the critical temperatures K_c and the amplitudes $\hat{D}$ and F_{1c}, above, have a

TABLE XXI. Values of the critical-point scattering parameters.

Heisenberg spin	Lattice	$\hat{D}$	ϕ_c^{η}	ϕ_c
∞	fcc	4.40±5	0.913±10	0.118
	bcc	4.27±5	0.910±10	0.110
	sc	3.92±5	0.906±10	0.100
$\frac{5}{2}$	fcc	4.32±5	0.908±10	0.103
	bcc	4.11±6	0.896±15	0.075
	sc	3.71±6	0.875±15	0.043
$\frac{3}{2}$	fcc	4.19±6	0.897±13	0.078
	bcc	3.97±7	0.883±18	0.055
	sc	3.51±7	0.849±18	0.022
1	fcc	4.00±7	0.879±15	0.049
	bcc	3.75±9	0.862±20	0.031
	sc	3.19±9	0.803±25	0.0059
$\frac{1}{2}$	fcc	3.34±20	0.80±5	0.0054
	bcc	3.11±30	0.79±9	0.0042
	sc	2.64±30	0.75±8	0.001
Ising $S=\frac{1}{2}$ (revised)	fcc	4.446±9	0.903±3	0.16
	bcc	4.305±15	0.903±4	0.16
	sc	3.98 ±2	0.897±5	0.14

clear lattice dependence (even in reduced form) and are *not* universal. Recently, Watson[28] and Kadanoff[29] have stressed the possibility that once these "normalization" factors have been chosen not only the exponents but also the scaling function itself should be "universal" (for a related class of systems). In the present case the normalization parameter F_{1c} is fixed via imposition of a unit coefficient of y^{-2} in (7.3), so that the only *shape parameter* determining the scaling function is ϕ_c. The complete universality hypothesis would thus suggest that a common value of ϕ_c should apply to all cases.

This conjecture is confirmed for the two-dimensional Ising model by the discovery that $\phi_c = 0.02940$ gives closest fits for *both* the square and triangular lattices.[3] In these cases the exact critical temperatures are known, which is a great aid to reliable extrapolation. For the three-dimensional models it is more meaningful to compare the estimates of ϕ_c^η [which is almost proportional to $D \simeq \Gamma_c^{xx}(\vec{\delta})$] since raising this to the $1/\eta \simeq 20$ power to find ϕ_c greatly magnifies the uncertainties. Equally, the actual magnitudes of the scattering curves vary mainly as ϕ_c^η rather than as ϕ_c. Reference to Table XXI shows that for the three $S=\infty$ Heisenberg lattices the value of ϕ_c^η lies within 0.5% of 0.910; this is well within the uncertainties of about 1%. Similarly the revised estimates of ϕ_c^η for the $S=\frac{1}{2}$ Ising lattices lie within 0.4% of 0.900 which is again closer than the extrapolation uncertainties. These results are rather strong support for the complete universality hypothesis, at least as regards independence of lattice structure. Not surprisingly, the values for the Heisenberg and Ising models *do* seem to differ significantly (although not by as much as they both deviate from the *two*-dimensional Ising value $\phi_c^\eta \simeq 0.414$). Recently Ferer, Moore, and Wortis[21] have also checked the universality hypothesis for the three-dimensional Ising models by a detailed comparison of the amplitudes for moments of differing orders above T_c. This approach is effectively complementary to ours since ϕ_c is determined through the correlation behavior *at* T_c. For spin $\frac{1}{2}$, Ferer, Moore, and Wortis confirm the validity of universality. In addition, for the fcc lattice they also presented evidence for universality with respect to the spin values $S=\frac{1}{2}, 1, \ldots, \infty$.

Turning next to the spin dependence in the Heisenberg model the situation is somewhat less clear. For the fcc lattice with $S \geq \frac{3}{2}$ all estimates are consistent with the value of ϕ_c^η of 0.910 for the $S=\infty$ lattices; but, even recognizing the appreciably larger uncertainties for $S=1$ and $S=\frac{1}{2}$, the low spin values appear to be some 3 and 12% lower. For a given spin the agreement between the three lattices is somewhat closer than this but for $S<2$ the differences again seem significant, with a monotonic dependence on coordination number reminiscent of

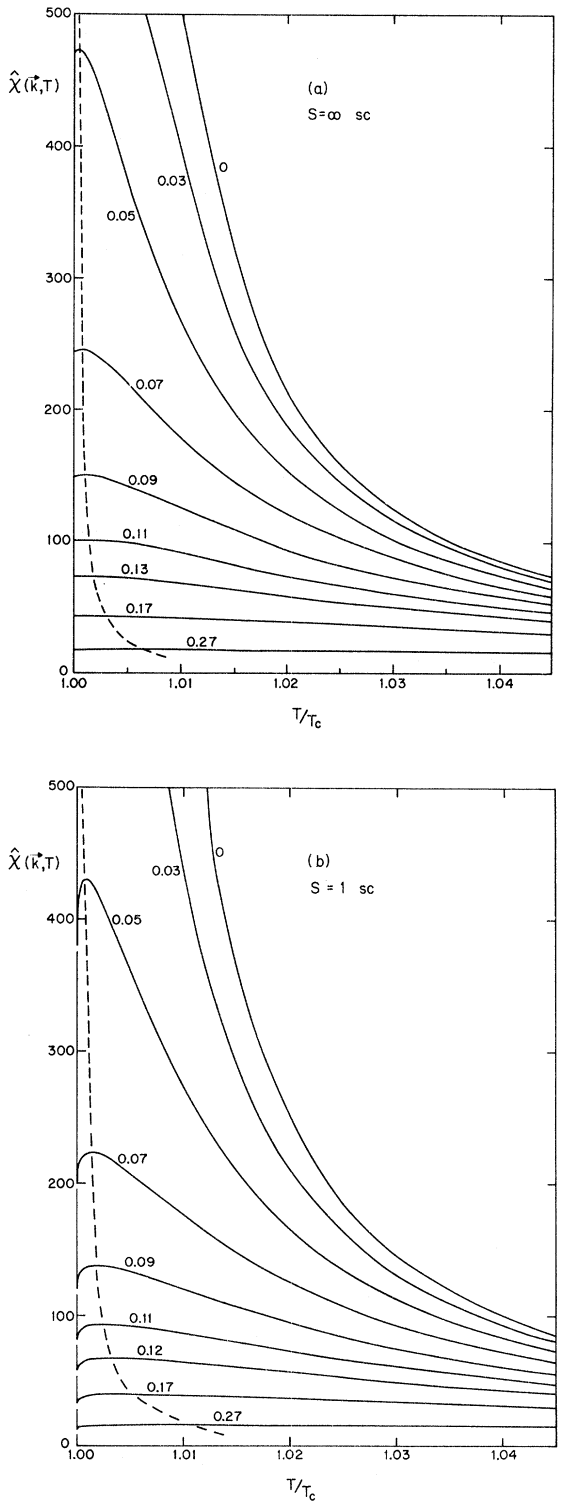

FIG. 10. Scattering intensity $\hat{\chi}(\vec{k}, T)$ as a function of temperature for various values of momentum transfer on the simple cubic lattice with spin values (a) $S=\infty$ and (b) $S=1$. The curves are labeled with the value of $k_x a$; the momentum transfer is taken parallel to the principal diagonal, i.e., $k_x = k_y = k_z$.

that seen in the amplitudes A_c, D, and F_{1c}, etc. (even according to the Bethe approximation[3]). It is certainly possible that these differences reflect a breakdown of complete universality in the quantum-mechanical cases of finite spin (as against the "classical" models $S=\infty$ Heisenberg and $S=\frac{1}{2}$ Ising model). On the other hand, it must also be recognized that the series data available for finite S are both less extensive and less regular than for $S=\infty$. Consequently, the systematic errors of extrapolation may well be somewhat larger than the apparent uncertainties (which, as usual, are mainly an indication of the internal and mutual consistency of different numerical techniques).

B. Scattering Curves

In Fig. 10, we have plotted the reduced scattering intensity $\hat{\chi}(\vec{k}, T)$ vs T for fixed $\vec{k}$ ($k_x a = k_y a = k_z a$) for simple-cubic Heisenberg model with $S=\infty$ and $S=1$. Figure 11 contains a similar plot for the sc lattice but for a range of spin values: For small ka the curves for low spin lie higher but for larger ka (or T closer to T_c) the low-spin plots drop below the higher-spin results. In Fig. 12, the (revised) curves for the $S=\frac{1}{2}$ Ising model are shown for the fcc, bcc, and sc lattices. Lastly, the dependence on lattice structure can be gauged from Fig. 13 where the $S=\frac{3}{2}$ data are plotted for the fcc, bcc,

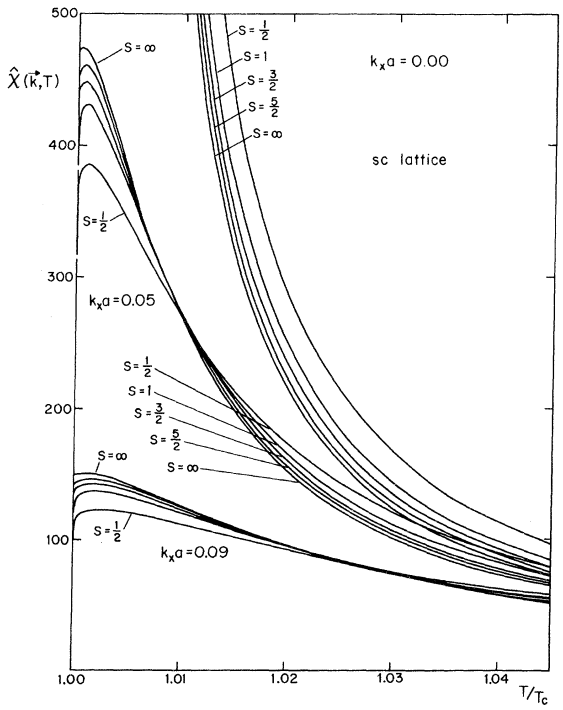

FIG. 11. Spin-dependence of the scattering curves. The scattering intensity is plotted as a function of temperature for $k_x a = 0$, 0.05, and 0.09 and spin values $S=\frac{1}{2}$, 1, $\frac{3}{2}$, $\frac{5}{2}$, and ∞.

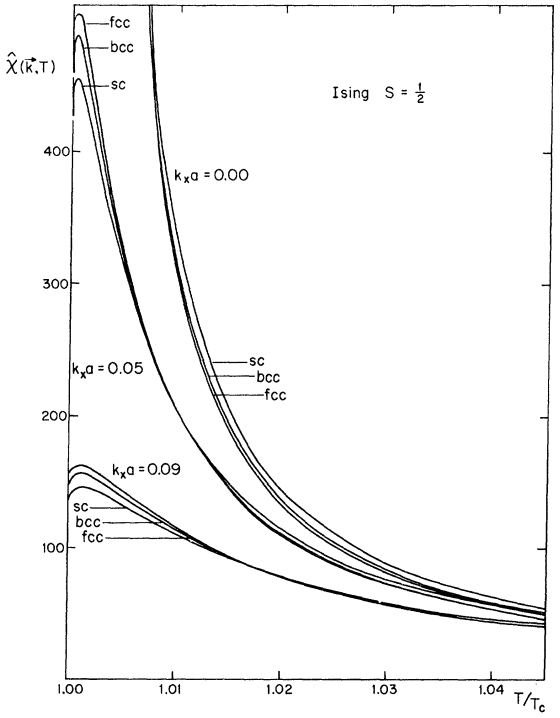

FIG. 12. Scattering curves for the Ising model, using revised estimates for ϕ_c. The scattering intensity is shown as a function of temperature for $k_x a = 0$, 0.05, and 0.09 for the fcc, bcc, and sc lattices. Again, the momentum transfer is parallel to the principal diagonal ($k_x a = k_y a = k_z a$).

and sc lattices. The variations with spin and lattice structure are not very marked, although they seem significant relative to the numerical uncertainties which may reach one or two percent for finite ka although they are probably less than $\frac{1}{2}\%$ for $ka < 0.07$, $T/T_c > 1.001$, and $S \geq 1$.

The most striking feature of the scattering curves is, as for the Ising model, the occurrence of a maximum in the scattering at fixed $\vec{k}$ at a temperature T_{max} which lies significantly *above* T_c. (As stressed by Fisher and Burford, this contrasts strongly with the predictions of Ornstein-Zernike and mean-field or random-phase approximations.) The deviation of T_{max} from T_c at a given $\vec{k}a$ increases monotonically as the spin or the coordination number is decreased. The value of T_{max}/T_c for the Heisenberg model is greater than for the corresponding Ising model. For sufficiently small ka the maximum of the scattering follows from (6.1) as[30]

$$(T_{max} - T_c)/T_c \approx [(\eta\psi_c - 2\phi_c^2)/(2-\eta)F_{1c}^2]^{1/2\nu}(ka)^{1/\nu}. \tag{7.4}$$

The actual calculated maxima for the various lattices are plotted vs $(ka)^{1/\nu}$ in Fig. 14. It can

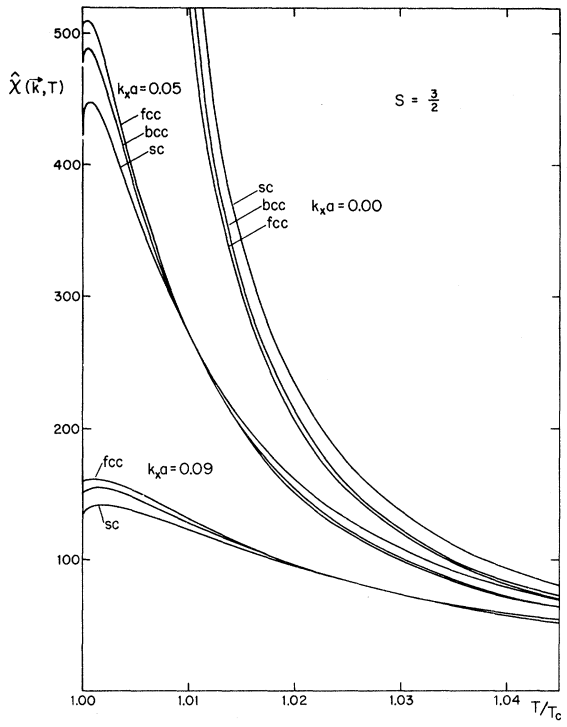

FIG. 13. Variation of the scattered intensity with lattice. The scattering curves are shown for the $S=\frac{5}{2}$ Heisenberg model on the fcc, bcc, and sc lattices.

be seen that the linear relation (7.4) only holds accurately for $ka \lesssim 0.04$. It must be pointed out that the precise position of the maximum is quite sensitive to the value of ϕ_c as is evident from (7.4). Thus the curves in Fig. 14 (especially for low spin) are much less firm than the scattering intensities themselves; however, we expect the general magnitudes and trends to be reliable. In particular, unless $\kappa_1(T)/k$ is equal to or less than 0.1 to 0.15, significant deviations from the simple Ornstein-Zernike form ($\eta = 0$, $\phi_c = 0$) are unlikely to be seen.

Finally, in Fig. 15(a), we plot for the simple-cubic lattice with $S=\frac{3}{2}$ the reciprocal scattering intensity $1/\hat{\chi}(\vec{k}, T)$ vs $k_x a$ out to the zone boundary $k_x a = \pi$. These curves are quite similar to those for the Ising model found in Paper I; in particular, the "neutral point," where $\hat{\chi}(\vec{k}, T) = 1$, is displaced markedly from $ka = \frac{1}{2}\pi$ towards $ka = 0$ as $T \to T_c$. A comparison was made with Collins's numerical results[15] for the fcc lattice with $S=\frac{1}{2}$ based on the truncated high-temperature series for $\hat{\chi}(\vec{k})$ [his $S(\vec{k})$]. Even at $T = 2T_c$ we find that the neglected higher-order terms make an additional 10% contribution to the susceptibility at low $\vec{k}a$; at $T = 3.5\,T_c$ the discrepancy is reduced to about 3%. Figure 15(b) indicates the effect of spin on these plots. Notice that for $T > T_c$ and small ka the plots for small spin lie lower. Again some word of caution is appropriate: The approximant (6.1) is designed, and has been optimized numerically, to give best results for low ka. Accordingly, the values predicted for $ka \gtrsim 1$ will be less reliable. In Paper I this point was investigated more closely with the conclusion that the accuracy around the zone boundaries was appreciably better, even close to T_c, than might have been guessed. For $S > 1$, the situation is probably similar here but further work would be required to confirm it.

C. Conclusions and Experiments

The main conclusions from our study of the correlation functions of the isotropic Heisenberg model may be summarized as follows. The critical scattering should, first, be described by exponents $\gamma = 1.375^{+0.02}_{-0.01}$, for $\chi_0(T)$ the zero-angle intensity, $2\nu = 1.405^{+0.02}_{-0.01}$ for the inverse range of correlation $\kappa_1(T)$ determined from the low-angle scattering, and $\eta \simeq 0.043 \pm 0.014$ for the critical-point-scattering line shape. Second, as a function of temperature the scattering at fixed wave number should display a maximum above T_c at a temperature determined roughly by $\kappa_1(T_{max})/k \simeq 0.10$ to 0.15 (the lower value applies for $S \gtrsim 2$; for the spin-$\frac{1}{2}$ three-dimensional Ising models the value is about

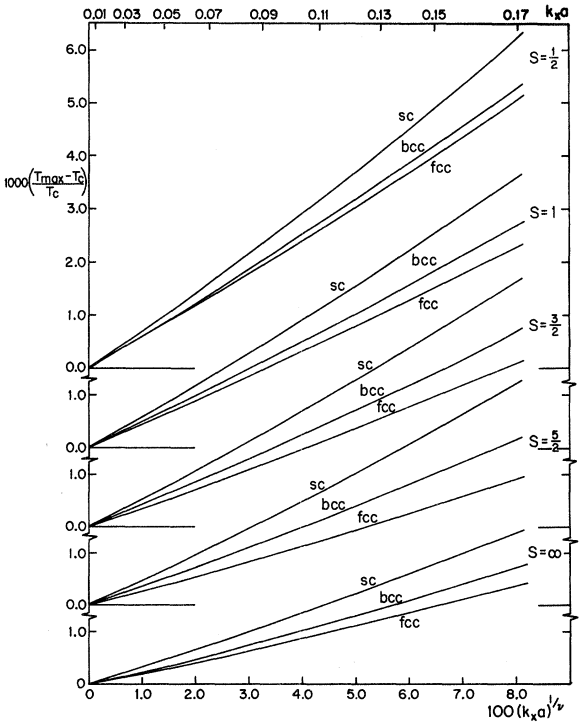

FIG. 14. Loci of the maximum $T_{max}(\vec{k})$ of the scattered intensity for all lattices and all spin values with $k_x = k_y = k_z$.

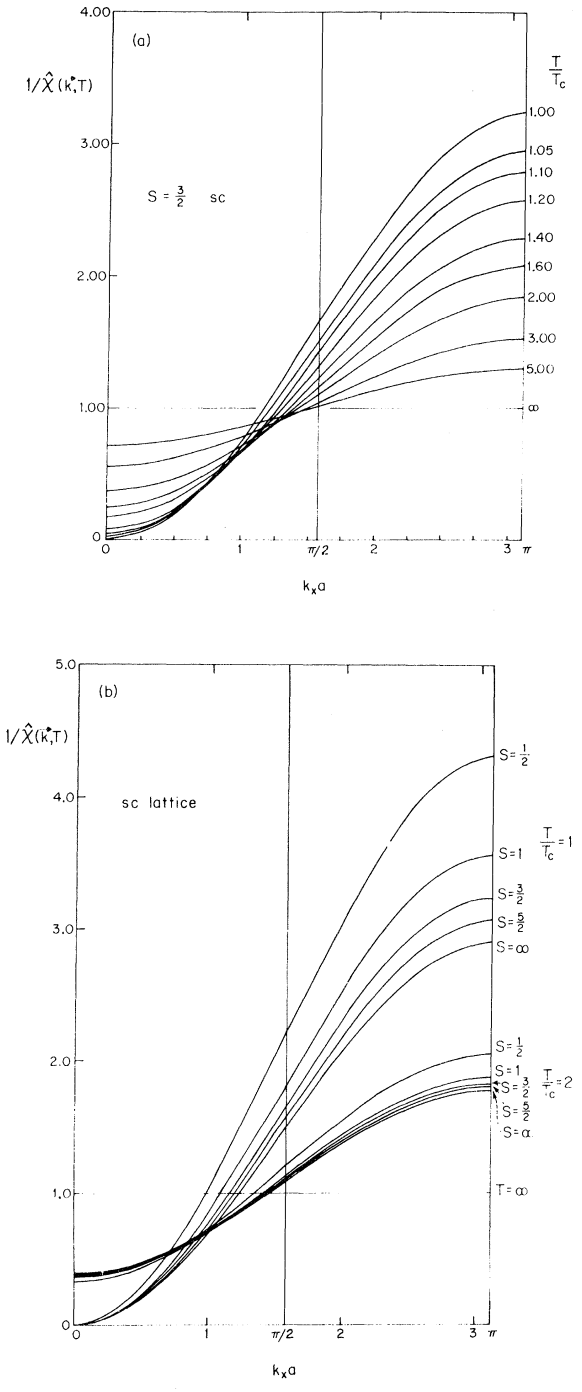

FIG. 15. Variation of the inverse scattered intensity with momentum transfer across the Brillouin zone. The inverse of the scattered intensity is plotted as a function of momentum transfer ($k_x a = k_y a = k_z a$) for (a) various values of T/T_c on the sc lattice with spin $S=\frac{3}{2}$ and (b) for $T=T_c$ and $T=2T_c$ for all the spin values $S=\frac{1}{2}$, 1, $\frac{3}{2}$, $\frac{5}{2}$, and ∞. Note the displacement of the neutral point $\hat{\chi}(\vec{k}, T) = 1$ from $k_x a = \pi/2$ to smaller values of $k_x a$; this displacement being more pronounced for T closer to T_c and for smaller spin values.

0.17). Conversely, for κ_1/k with significantly larger values than these, the scattering should fit quite well to a Lorentzian or Ornstein-Zernike form. (A guide to the calculation of the detailed scattering function is given in the summary at the end of Sec. VI.)

We have not undertaken a detailed comparison of these conclusions with available experimental evidence. It is appropriate, nonetheless, to mention a few salient experiments. Recently, Popovici[31] has reexamined the data from earlier two-axis-spectrometer critical-neutron-scattering experiments on iron by Bally *et al.*[32] in the light of general criticisms by Als-Nielsen[33] concerning the importance of proper inelasticity corrections. The new analysis[31] indicates $\gamma = 1.345 \pm 0.02$, $2\nu = 1.38 \pm 0.04$, which values are somewhat lower than the Heisenberg model estimates, although much closer to them than to the Ising values of $\gamma = 1.25$ and $2\nu \simeq 1.285$. (Of course, iron cannot, in any case, be regarded as a good example of a system with localized Heisenberg spins.) By direct fit to the scattering at T_c, Popovici[31] concludes that $\eta = 0.10 \pm 0.05$. In view of the residual uncertainties involved in the inelasticity corrections this is in quite reasonable agreement with our results. Last, after the corrections, Popovici still observes the maxima at fixed $\vec{k}$ above T_c which were earlier reported.[32] The location of the maxima, however, is now in quite close accord with our predictions (for low spin) whereas in the first analysis the maxima were much too pronounced. Despite these encouraging results there is a clear need for other detailed experiments on ferromagnets.

Although the direct observation of η through a scattering experiment is rather hard it is worth stressing that indirect evidence indicating its positivity follows from the inequality[34,35]

$$2 - \eta \leq d(\delta - 1)/(\delta + 1) , \qquad (7.5)$$

in which d is the dimensionality and δ is the standard exponent describing the critical isotherm ($|M| \sim |H|^{1/\delta}$ at $T = T_c$). This inequality has been proven quite rigorously[35,36] on the basis of symmetry with respect to field inversion and the positivity and monotonicity with field of the spin-spin correlation functions of a ferromagnet near T_c. The evidence for most real ferromagnets[37] indicates strongly that $\delta \leq 4.7$; the inequality then unequivocally implies $\eta \geq 0.05$. Difficulties in observing the effects of positive η in scattering experiments must thus be attributed to lack of precision and to the technical problems of making proper resolution and inelasticity corrections or, partly, to the shape of the scaling function being such that non-Ornstein-Zernike behavior is only evident very close to T_c.

For an antiferromagnet in the classical limit $S = \infty$ our present calculations can be taken over di-

rectly if one merely replaces J by $|J|$ and $\vec{k}$ by $\vec{k}-\vec{k}_0$, where $\vec{k}_0$ is the zone-corner wave vector at which the antiferromagnetic-Bragg-scattering peak appears below T_c.[3] For finite S, quantum effects spoil this precise symmetry but, at least for the larger values of S, we may expect the results to be fairly similar to those for the ferromagnet. (We remark that for $S<\infty$ the antiferromagnetic critical temperatures are higher than those of the corresponding ferromagnets.[38]) Accordingly, the neutron scattering experiments by Corliss *et al.*[39] on $RbMnF_3$ are of particular interest, especially since the simple-cubic, nearest-neighbor $S=\frac{5}{2}$ Heisenberg Hamiltonian is known to describe this material rather closely.[40] The exponents reported by Corliss *et al.*[39] were $\gamma \simeq 1.397 \pm 0.034$ and $2\nu = 1.448 \pm 0.016$, which are somewhat higher than our estimates, although probably not really inconsistent with them. Close to T_c pronounced deviations from a Lorentzian line shape were observed; these were well fitted by the simple approximant $\hat{D}/[(\kappa_1 a)^2 + (ka)^2]^{1-\eta/2}$ with $\eta = 0.067 \pm 0.009$, which is consistent with $(2-\eta)\nu = \gamma$. This approximant was introduced earlier[2,3] and is not as accurate as the one developed here (Sec. VI) but is probably satisfactory for estimating η close to T_c. Again, although the observed and calculated ranges for η do not quite overlap we do not feel that the discrepancies are very significant. Experiments by Schulhof *et al.*[41] on the antiferromagnet MnF_2 yielded $\gamma = 1.24 \pm 0.02$ and $2\nu = 1.27 \pm 0.03$. These values are much lower than for $RbMnF_3$ and, indeed, essentially coincide with the Ising-model values which would be expected to apply to a significantly anisotropic system. However, deviations from Lorentzian scattering were again observed leading to the estimate $\eta = 0.05 \pm 0.02$; this is consistent with the theoretical estimates for both Ising and Heisenberg models. Finally, we may mention the experiments by Norvell *et al.*[42] on the Ising-like antiferromagnet, dysposium aluminum garnet (DAG) which lead to the even lower values[42] $\gamma = 1.16 \pm 0.04$ and $2\nu = 1.22 \pm 0.02$. These may, however, be associated with the important role of the long-range dipolar interactions in this material. Nevertheless, the nonzero value $\eta = 0.12 \pm 0.10$ was observed.

In summary there is quite good experimental evidence for most of the qualitative features of the critical scattering predicted by our calculations; in addition, the quantitative agreement is quite fair. There remains, however, scope for more extensive and detailed comparisons [for example, with the absolute magnitudes of $\kappa_1(T)$] and for further experiments, especially on ferromagnetic materials.

ACKNOWLEDGMENTS

We are indebted to Dr. M. A. Moore and Dr. David Jasnow for generously making much of their numerical data available to us. Dr. Jasnow also lent us detailed assistance. Professor Michael Wortis and Dr. G. A. Baker, Jr., kindly commented on the manuscript. The support of the National Science Foundation and of the Advanced Research Projects Agency through the Materials Science Center at Cornell University is gratefully acknowledged. The work was completed while the senior author held a John Simon Guggenheim Fellowship in the Applied Physics Department at Stanford University. The hospitality of Professor S. Doniach and the partial support of the U. S. Army Research Office, Durham, North Carolina was appreciated.

[1]L. Van Hove, Phys. Rev. 95, 249 (1954); 95, 1374 (1954).

[2]See, e.g., M. E. Fisher, (a) J. Math. Phys. 5, 944 (1964); (b) Rept. Progr. Phys. 30, 615 (1967).

[3]M. E. Fisher and R. J. Burford, Phys. Rev. 156, 583 (1967); see the errata noted in Ref. 30.

[4]N. D. Mermin and H. Wagner, Phys. Rev. Letters 17, 1133 (1966); D. Jasnow and M. E. Fisher, *ibid.* 23, 286 (1969); Phys. Rev. B 3, 907 (1971).

[5]H. E. Stanley and T. A. Kaplan, Phys. Rev. Letters 16, 981 (1966); J. Appl. Phys. 38, 975 (1967).

[6]Y. A. Izyumov, Usp. Fiz. Nauk 80, 41 (1963) [Sov. Phys. Usp. 6, 359 (1963)].

[7]W. Marshall and R. D. Lowde, Rept. Progr. Phys. 31, 705 (1968).

[8]G. S. Rushbrooke and P. J. Wood, Mol. Phys. 1, 257 (1958).

[9]R. L. Stephenson, K. Pirnie, P. J. Wood, and J. Eve, Phys. Letters 27A, 2 (1968).

[10]G. A. Baker, Jr., H. E. Gilbert, J. Eve, and G. S. Rushbrooke, Phys. Letters 20, 146 (1966).

[11]G. A. Baker, Jr., H. E. Gilbert, J. Eve, and G. S. Rushbrooke, Phys. Rev. 164, 800 (1967).

[12](a) D. Jasnow and M. Wortis, Phys. Rev. 176, 739 (1968); (b) D. Jasnow, Ph. D. thesis (University of Illinois, Urbana, 1969) (unpublished).

[13](a) M. A. Moore (private communication). We are indebted to Dr. Moore and the Illinois group for making the results of their work available to us. (b) Since this paper was submitted we have learnt of work by M. Ferer, M. A. Moore, and M. Wortis [Phys. Rev. B 4, 3954 (1971); 4, 3964 (1971)] in which these $S=\infty$ fcc series, as well as data on the field behavior, have been published and carefully analyzed by ratio methods. (c) Ferer *et al.* also observed that the Bowers-and-Woolf apparently rapid convergence was misleading. However, they concluded for the fcc lattice that $\gamma = 1.40$. We have reexamined our own analysis in the light of their arguments but are still inclined to estimate $\gamma = 1.38 \pm 0.001$, as in Table V. (d) Acceptance of the high estimate $\gamma = 1.40$ leads to an approximately modified critical-point estimate and an associated higher estimate of 2ν than we find. However, Ferer, Moore, and Wortis also conclude that $2\nu - \gamma \simeq 0.03$, so that their estimate for η is still in close agreement with ours.

[14]R. J. Burford, Ph. D. thesis (University of London,

1966) (unpublished). A preliminary analysis of some of Burford's data has been presented by M. E. Fisher, *Critical Phenomena*, Natl. Bur. Std. Misc. Publ. No. 273 (U.S. GPO, Washington, D.C., 1966); see also Ref. 2(b).

[15]M. F. Collins, Phys. Rev. B 2, 4552 (1970); see also a correction noted after Eq. (4) in Phys. Rev. B 4, 1588 (1971).

[16]See, e.g., M. E. Fisher, *The Nature of Critical Points Lectures in Theoretical Physics VII* (University of Colorado Press, Boulder, Colorado, 1965), pp. 73–109.

[17]G. S. Joyce and R. G. Bowers, Proc. Phys. Soc. (London) 89, 776 (1966).

[18]C. Domb and M. F. Sykes, Phys. Rev. 128, 168 (1962).

[19]R. G. Bowers and M. E. Woolf, Phys. Rev. 177, 917 (1969).

[20]P. F. Fox and A. J. Guttmann, Phys. Letters 31A, 234 (1970); P. F. Fox and D. S. Gaunt, J. Phys. C 3, 188 (1970).

[21]M. Ferer, M. A. Moore, and M. Wortis, Phys. Rev. B 3, 3911 (1971).

[22]R. L. Stephenson and P. J. Wood, (a) Phys. Rev. 173, 475 (1968); (b) J. Phys. C 3, 90 (1970).

[23]C. Domb and R. G. Bowers, J. Phys. C 2, 755 (1969).

[24]H. E. Stanley, J. Appl. Phys. 40, 1272 (1969).

[25]See, e.g., Refs. 12; the technique was first introduced in the context of series expansions by G. S. Rushbrooke but it should be noted that here we are extrapolating partial sums rather than coefficient ratios (for which we feel the technique has less validity).

[26]A. A. Maradudin, E. W. Montroll, G. H. Weiss, R. Herman, and H. W. Milnes, Acad. Roy. Belg. Sci. 14, 7 (1960).

[27]I. Mannari and C. Kawabata, Research Notes of the Department of Physics Okayama University, Okayama, Japan, No. 15, 1964 (unpublished).

[28]P. G. Watson, J. Phys. C 2, 1883, 2158 (1969).

[29]L. P. Kadanoff, Nuovo Cimento Suppl. (to be published).

[30]Note that a factor of 2 is missing from the ϕ_c^2 term in Eq. (11.14) of Paper I. Other corrections to Paper I are: in Eq. (9.3) the sign of $\ln|t|$ should be negative; in the lower half of Table XI the heading (2, 1, 0) should read (2, 1, 1); in Eq. (11.8) horizontal rules under a^3 and a are missing. Professor K. G. Wilson, in a recalculation of Eq. (7.18), finds the last coefficient should be 16 140 (in place of 16 124). This correction makes small numerical changes in the subsequent numerical analysis but will not alter any conclusions significantly. The numerical coefficient in Eq. (11.8) should read 12.9605. (We are grateful to Dr. M. Ferer for having helped us uncover this error.) The corrected equation leads to changes in the estimates for $\hat{D}$ and ϕ_c for the three-dimensional lattices; however, these estimates are in any case superseded by those given in Table XXI of the present paper.

[31]M. Popovici, Phys. Letters 34A, 319 (1971).

[32]D. Bally, M. Popovici, M. Totia, B. Grabcev, and A. M. Lungu, J. Appl. Phys. 39, 459 (1968); Phys. Letters 26A, 396 (1968).

[33]J. Als-Nielsen, Phys. Rev. Letters 25, 730 (1970).

[34]J. D. Gunton and M. J. Buckingham, Phys. Rev. Letters 20, 143 (1967).

[35]M. E. Fisher, Phys. Rev. 180, 594 (1969).

[36]M. J. Buckingham and J. D. Gunton, Phys. Rev. 178, 848 (1969).

[37]See, e.g., A. Arrott and J. E. Noakes, Phys. Rev. Letters 19, 786 (1967); J. S. Kouvel and J. B. Comly, *ibid.* 20, 1237 (1968); K. Miyatani, J. Phys. Soc. Japan 26, 259 (1969); J. T. Ho and J. D. Litster, Phys. Rev. 2, 4523 (1970); M. Vicentini-Missoni, R. I. Joseph, M. S. Green, and J. M. H. Levelt-Sengers, Phys. Rev. B 1, 2312 (1970).

[38]See Ref. 2(b), p. 701; G. S. Rushbrooke and P. J. Wood, Mol. Phys. 6, 409 (1963).

[39]L. M. Corliss, A. Delapalme, J. M. Hastings, H. Lau, and R. Nathans, J. Appl. Phys. 40, 1278 (1969).

[40]See, e.g., C. G. Windsor, G. A. Briggs, and M. Kestigan, J. Phys. C 1, 940 (1968).

[41]M. P. Schulhof, P. Heller, R. Nathans, and A. Linz, Phys. Rev. B 1, 2304 (1970).

[42]J. C. Norvell, W. P. Wolf, L. M. Corliss, J. M. Hastings, and R. Nathans, Phys. Rev. 186, 567 (1969).